JOURNAL OF TRAFFIC AND TRANSPORTATION ENGINEERING (ENGLISH EDITION) 2024; 11 (6): 1210–1242

Available online at www.sciencedirect.com

ScienceDirect

journal homepage: www.keaipublishing.com/jtte

Review Article

Evaluation of fatigue life of asphalt binders using the time sweep and linear amplitude sweep tests: A literature review

Mohammed Nouali [a,*], *Anne Dony* [a], *Alan Carter* [b]

[a] *Institut de Recherche, ESTP: Grande école d'ingénieurs de la construction, Cachan 94230, France*

[b] *Laboratoire sur les chaussées et matériaux bitumineux, École de Technologie Supérieure ETS, Montréal, QC H3C 0J8, Canada*

HIGHLIGHTS

- LAS test is now the preferred method for assessing asphalt binders fatigue life.
- The VECD concept is extensively used to analyze LAS test data.
- The G^R approach has become the most favored method for analyzing the LAS test.
- Fatigue test temperature significantly impacts the fatigue life of asphalt binders.
- Softer binders and polymer-modified binders demonstrate higher fatigue resistance.

ARTICLE INFO

Article history:
Received 30 December 2023
Received in revised form
12 April 2024
Accepted 17 April 2024
Available online 5 December 2024

Keywords:
Asphalt binder
Fatigue test
Failure criterion
TS test
LAS test
Viscoelastic continuum damage

ABSTRACT

Asphalt binders play a crucial role in the fatigue cracking resistance of asphalt pavement, making the characterization of their fatigue life increasingly important. To evaluate the fatigue life of asphalt binders, two tests have been developed: the time sweep (TS) and the linear amplitude sweep (LAS), both conducted using the dynamic shear rheometer (DSR). Similar to asphalt mixtures, predicting the fatigue life of asphalt binders necessitates the predefinition of fatigue failure criterion and/or fatigue failure definition (failure point). Phenomenological and dissipated energy-based failure criteria are commonly employed to analyze TS test results, while the viscoelastic continuum damage (VECD) model is primarily used to predict fatigue life through the LAS test. Given that the fatigue test temperature significantly impacts the fatigue life of asphalt binders, various methods have been proposed in the literature for selecting the fatigue test temperature.

This paper provides a comprehensive review of the fatigue life evaluation of asphalt binders using both TS and LAS tests. It summarizes the different fatigue failure criteria and fatigue failure definitions employed and discusses the selection of fatigue test temperatures. Furthermore, the paper examines the influence of fatigue test conditions, binder chemical composition and/or penetration grade, and bitumen modification on the fatigue life of asphalt binders. Based on the current review, it is recommended to utilize the LAS test on PAV-aged bitumen under strain-controlled conditions to evaluate the fatigue life of asphalt binders. The most relevant failure definition is the peak in stored pseudo-strain energy based on the simplified viscoelastic continuum damage model (S-VECD).

* Corresponding author.
E-mail addresses: mnouali@estp.fr (M. Nouali), adony@estp.fr (A. Dony), Alan.Carter@etsmtl.ca (A. Carter).

Peer review under responsibility of Periodical Offices of Chang'an University.
https://doi.org/10.1016/j.jtte.2024.04.007

Additionally, the authors propose conducting the fatigue test at an intermediate reference temperature for each country or region, depending on its climate zone.

Nomenclature

A	Material dependent parameters
B	Material dependent parameters
BYET	Binder yield energy test
C	Material integrity (pseudo-stiffness)
CDER	Cumulative dissipated energy ratio
CR	Crumb rubber
CSR	Constant strain-amplitude rates
D	Damage variable
D_f	Damage at failure
DCCs	Damage characteristic curves
DER	Dissipated energy ratio
DMR	Dynamic modulus ratio
DSR	Dynamic shear rheometer
ER	Energy ratio
E_R	Reference modulus
f	Frequency
FS	Frequency sweep
G^*	Complex shear modulus
$\|G^*\|_{initial}$	Initial dynamic shear modulus
$\|G^*\|_{LVE}$	Linear dynamic shear modulus
G^R	Averaged release rate of PSE
HPMB	Highly polymer modified binder
i	Cycle number
Ic	Colloidal instability index
LAS	Linear amplitude sweep
LVE	Linear viscoelastic
m	Slop of the log-log plot of relaxation with time
NCHRP	National cooperative highway research program
N_f	Fatigue life
NLVE	Nonlinear viscoelastic
N_p	Number of cycles to reach the crack propagation
NSR	Normalized stiffness ratio
PAV	Pressurized aging vessel
PG	Performance grade
PPA	Peak phase angle
PSE	Pseudo-strain energy
PSS	Peak shear stress
PSPSE	Peak stored PSE
PV	Plateau value
RDEC	Ratio of dissipated energy change
RTFOT	Rolling thin-film oven test
SBS	Styrene-butadiene-styrene
SHRP	Strategic highway research program
SR	Stiffness ratio
T°	Temperature
t	Time
TS	Time sweep
VECD	Viscoelastic continuum damage
W	Dissipated energy
W^R	Pseudo-strain energy density
W^R_{Total}	Total PSE
$\overline{W^R_r}$	Averaged released PSE
W^R_r	Released PSE
W^R_s	Stored PSE
α	Damage evolution rate
a_T	Time-temperature shift factor
γ	Strain amplitude
δ	Phase angle
σ_i	Shear stress at cycle i
σ_p	Peak shear stress at cycle i
ϵ_i	Shear strain at cycle i
${\epsilon^R}_i$	Pseudo strain
ϵ^R_p	Peak shear pseudo strain
ξ	Reduced time

1. Introduction

Under repeated loading, all asphalt materials accumulate damage (Ghuzlan and Carpenter, 2006; Jia et al., 2023), leading to potential fatigue cracking in asphalt pavements. Damage accumulation primarily involves the degradation of mechanical properties due to the growth of microcracks within the material (Johnson, 2010; Sudarsanan and Kim, 2022). As damage accumulates, the materials don't need higher stress to increase or maintain the strain, indicating a significant change in material integrity and ultimately leading to fatigue failure (Roque et al., 2020). According to the literature, several parameters can affect the fatigue of asphalt pavements, including the layer thickness, layer interface conditions, the physical and chemical properties of the asphalt binders, the binder content, the binder aging, and etc. (Alae et al., 2020; NCHRP, 2021; Sudarsanan and Kim, 2022; Wang et al., 2017). In asphalt pavements, there are two main fatigue-cracking mechanisms, bottom-up and top-down cracking (Canestrari and Ingrassia, 2020; NCHRP, 2021; Roque et al., 2020). The bottom-up fatigue cracking originates at the bottom of the hot mix asphalt layer due to the high tensile strain created by repeated load cycles and progresses upward. Conversely, the top-down fatigue cracking (longitudinal cracks near the wheel paths) originates at the surface and progressively propagates downward through the asphalt layer. It can evolve in three stages: single crack, sister cracks, alligator cracking (Canestrari and Ingrassia, 2020). In both mechanisms, fatigue cracking initiates through the binder-aggregate interface or mastic and gradually propagates until failure (Hammoum et al., 2002; Maillard, 2002). The asphalt binder is considered to be the main factor controlling fatigue cracking of the asphalt mixture since it is the only viscoelastic material within the asphalt mixture (Shen et al., 2006). Laboratory tests reveal the fatigue damage mechanism in asphalt concrete in three phases, illustrated in Fig. 1 (Lefeuvre, 2001; Piau, 1989).

- Phase I (pre-localization phase) involves the initiation and propagation of microcracks, with a rapid stiffness reduction attributed to thixotropy and sample heating.
- Phase II (localization phase) is characterized by the interaction and coalescence of micro-cracks (stress concentration), leading to a linear decrease in stiffness due to fatigue damage (continuum damage state).
- Phase III (post-localization phase) is characterized by the propagation of macro-cracks (failure of material) (Di Benedetto et al., 2004; Perraton et al., 2003). The localization phase is the transition region between the distributed micro-cracks (pre-localization) and localized macro-cracks (post-localization).

The three stages are widely investigated using the continuum damage models (phases I and II) and fracture models (phase III).

The viscoelastic continuum damage model (VECD), initially proposed and developed by Schapery (1984), is mostly used in quantifying the evolution and growth of damage in viscoelastic materials (phases I and II). However, for the post-localization phase (phase III), characterized by nonlinear behavior and intense damage, is investigated using fracture mechanics.

Numerous tests and methods have been adopted to characterize the fatigue life of asphalt materials under repeated loading. As previously mentioned, the asphalt binder is the principal component in the asphalt mixtures responsible for the damage and fatigue cracking of asphalt pavement. Consequently, since 2001, there has been a growing interest in characterizing the fatigue life of asphalt binders. Initially, the $G^*\sin(\delta)$ parameter was introduced by the Strategic Highway Research Program (SHRP) to evaluate the fatigue resistance of asphalt binders. $G^*\sin(\delta)$ represents the viscous component of the complex shear modulus, serving as an indicator of total dissipated energy and it must not exceed a certain value for adequate fatigue resistance. Criticism of the $G^*\sin(\delta)$ fatigue indicator has been significant in literature, primarily because no damage is expected to occur in the linear viscoelastic domain (LVE) (Bahia et al., 2001; Bessa et al., 2019; Johnson, 2010). In 2001, Bahia et al. (2001) proposed the time sweep (TS) test, within the framework of NCHRP 9-10, to evaluate the fatigue life of asphalt binders under repeated sinusoidal loading (strain or stress-controlled mode) using the dynamic shear rheometer (DSR). However, due to the time-consuming nature of the TS test, Johnson et al. (2009) introduced the binder yield energy test (BYET) using DSR. The BYET evaluates the yield energy and the strain corresponding to the peak shear stress ($\gamma_{\tau max}$), serving as indicators for asphalt fatigue. In 2010, Johnson and Bahia (2010) developed the linear amplitude sweep (LAS) test to predict the fatigue life of asphalt binders using the DSR, as detailed in section 2. The LAS test data are interpreted based on the VECD modeling principle.

Regardless of the fatigue test employed, studying the fatigue life of asphalt binders and asphalt mixtures necessitates a predefined failure criterion and/or failure definitions (failure point). According to Zhang et al. (2013), the failure definition is the transition point between the viscoelastic continuum damage and fracture regimes. Several failure criteria and failure definition have been proposed and investigated to predict the fatigue life of both asphalt mixtures and binders. The failure criteria can be broadly categorized into the phenomenological failure criteria (detailed in subsection 3.1) and dissipated energy-based failure criteria (described in subsection 3.2) (Chen et al., 2022; Zeiada et al., 2022). Importantly, the same failure criteria are applicable for both asphalt mixtures and binders. It is worth noting that the test temperature significantly influences the fatigue life of asphalt binders. Various temperatures have been selected and tested in the literature to evaluate the fatigue life of asphalt binders using both TS and LAS tests (detailed in subsection 7.1).

This paper reviews the state of the art related to the evaluation and prediction of the fatigue life of asphalt binders focusing on the time sweep and linear amplitude sweep tests. It is noteworthy that the study of the fatigue of asphalt binders remains, up to date, limited compared to the asphalt mixtures.

In total, 81 research papers on asphalt binder fatigue using TS and LAS tests have been thoroughly reviewed. Fig. 2 illustrates the distribution of these papers by year, revealing a consistent annual increase since 2015. Notably, research from the USA and China dominates, representing a significant portion of the reviewed papers, as depicted in Fig. 3. Specifically, among the 81 reviewed papers, 56 originate from the USA and China, comprising approximately 69% of the total. Conversely, the study of asphalt binder fatigue in Europe and Africa remains relatively limited.

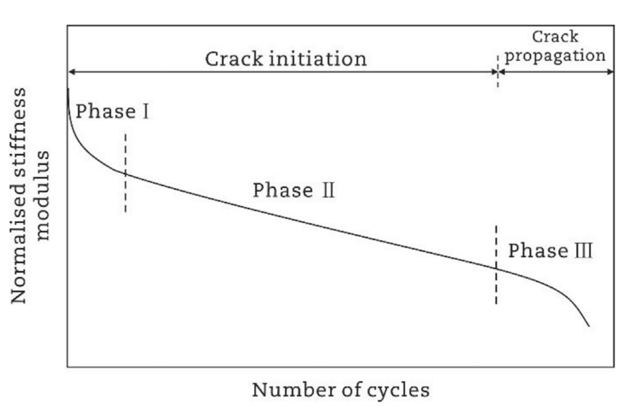

Fig. 1 – The fatigue damage mechanism in asphalt concrete (Ahmed et al., 2019).

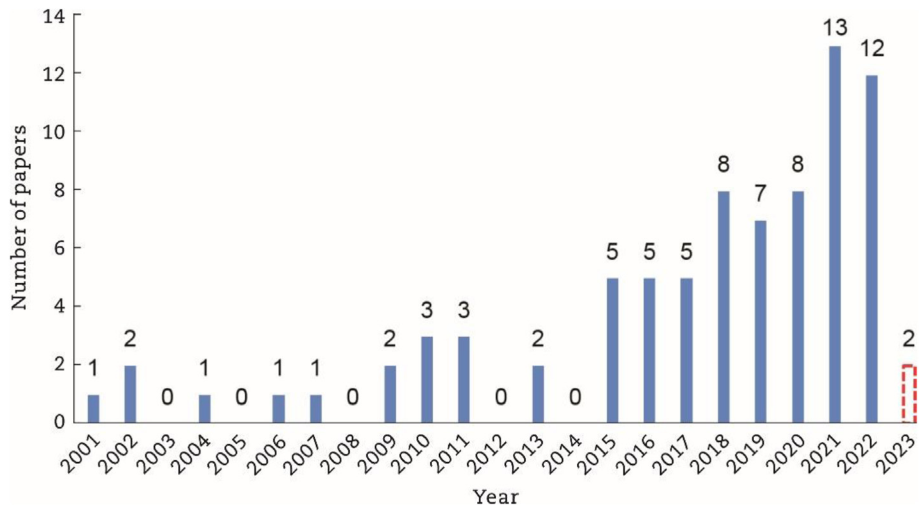

Fig. 2 – Distribution of the 81 reviewed papers by year of publication.

From the 81 reviewed research papers, 33 research papers exclusively utilized the LAS test to evaluate the fatigue life of asphalt binders, which corresponds to 40.7%, as indicated in Fig. 4. Additionally, 28 research papers (34.6%) relied solely on the TS test, while 17 research papers (21%) employed both TS and LAS tests. However, only 3 research papers (Johnson et al., 2009; Morshed et al., 2020; O'Connell et al., 2017) utilized the BYET test as an indicator of the fatigue of asphalt binders.

In summary, the process for evaluating the fatigue life of asphalt binders using the TS and LAS tests is summarized in Fig. 5. As per literature recommendations, asphalt binders should undergo aging via the rolling thin film oven test (RTFOT) and pressure aging vessel (PAV) procedures and then characterized to determine their undamaged linear viscoelastic properties. Whatever the fatigue test used, it is crucial to carefully select the fatigue test temperature, as it significantly impacts fatigue life, and the adopted failure criterion and failure definition also plays a crucial role in determining asphalt binder fatigue life. This review paper emphasizes the various failure criteria and failure definitions utilized in analyzing TS and LAS fatigue tests. Additionally, it examines the influence of fatigue test temperature, asphalt binder chemical composition and/or penetration grade, and bitumen modification on asphalt binder fatigue life.

2. Tests and methods used to evaluate the fatigue of asphalt binders

Until now, the G*sin(δ) parameter has been widely used as an indicator for the fatigue behavior of binders (AASHTO, 2015). Initially, the G*sin(δ) value, measured after PAV at 10 rad/s (1.59 Hz) and 1% strain amplitude, was limited at 3000 kPa. Actually, the Superpave specification (AASHTO, 2015) required that the G*sin(δ) parameter, after PAV test, must not exceed 5000 kPa at a frequency of 10 rad/s for standard traffic and 6000 kPa for heavy and very heavy traffic (AASHTO, 2015). This fatigue indicator has been largely criticized for the reason that the test is conducted within the linear viscoelastic domain (Bahia et al., 2001; Bessa et al., 2019; Johnson, 2010), whereas asphalt binders fatigue damage occurs in the non-linear viscoelastic domain. In response to the lack of correlation between the G*sin(δ)

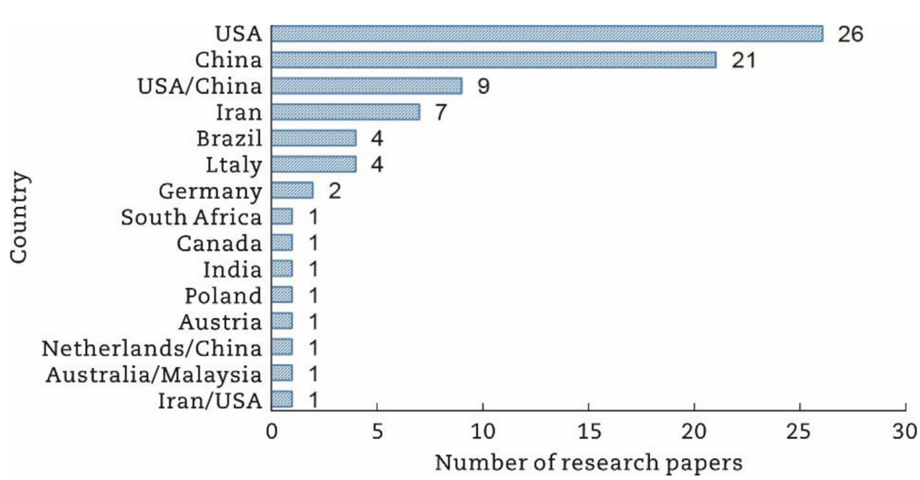

Fig. 3 – Number of reviewed research paper per country.

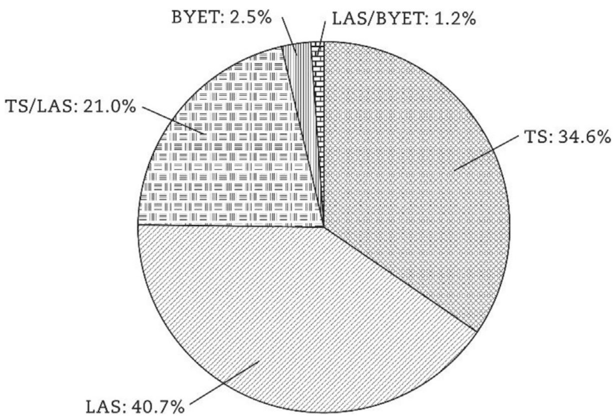

Fig. 4 – Repartition of the utilization of the TS, LAS and BYET in the reviewed papers.

Superpave fatigue parameter and fatigue of asphalt mixture, new fatigue binder tests were developed. In 2001, Bahia et al. (2001) introduced the TS test to evaluate the fatigue of asphalt binder using a DSR (8 mm parallel plates with 2 mm gap) by means of the degradation of material integrity under cyclic loading. The TS can be conducted under controlled stress or strain at a constant frequency and amplitude by applying of cyclic loading. It is necessary that the stress or strain levels selected, to perform the TS fatigue test, are outside of the linear viscoelastic region due to the non-linear damage behavior of asphalt binders. To be outside the linear viscoelastic region of the binder, the selected strain level for the test must be equal or higher than the strain level required to have 5% reduction of the initial complex modulus (Airey and Rahimzadeh, 2004). Based on this principle, Nan et al. (2022) recommended using the stress/strain LVE limit as the applied amplitude for conducting the time sweep test. The strain level must be carefully chosen, as high-performance asphalt binder may not fail under a small strain level, while weaker asphalt can be significantly damaged under a high strain level (Yan et al., 2022). As an indication, Martono and Bahia (2008) and Bessa et al. (2019) conducted the TS tests at a different strain levels, ranging from 2% to 10% strain. The choice of the testing frequency does not have a significant impact on the fatigue life (Boussabnia et al., 2021), but it does have an impact on the test duration. The time sweep test is considered time-consuming, especially when different strain amplitudes are tested. For one strain amplitude, the total testing time is around 16 h (576,000 cycles) (Anderson et al., 2001). In order to perform the time sweep test within a reasonable time (30 min–6 h), Yan et al. (2022) suggested selecting the strain amplitude between 2% and 6% using a 10 Hz loading frequency. Tabatabaee and Tabatabaee (2010) demonstrated that most tested binders did not fail within a reasonable time under 1.59 Hz and 10% strain compared to those tested at 15 Hz. Due to the long duration of the TS test, alternative fatigue tests have been developed to evaluate the fatigue life of asphalt binders in a reasonable time using the DSR. In 2009, Johnson et al. (2009) introduced the binder yield energy

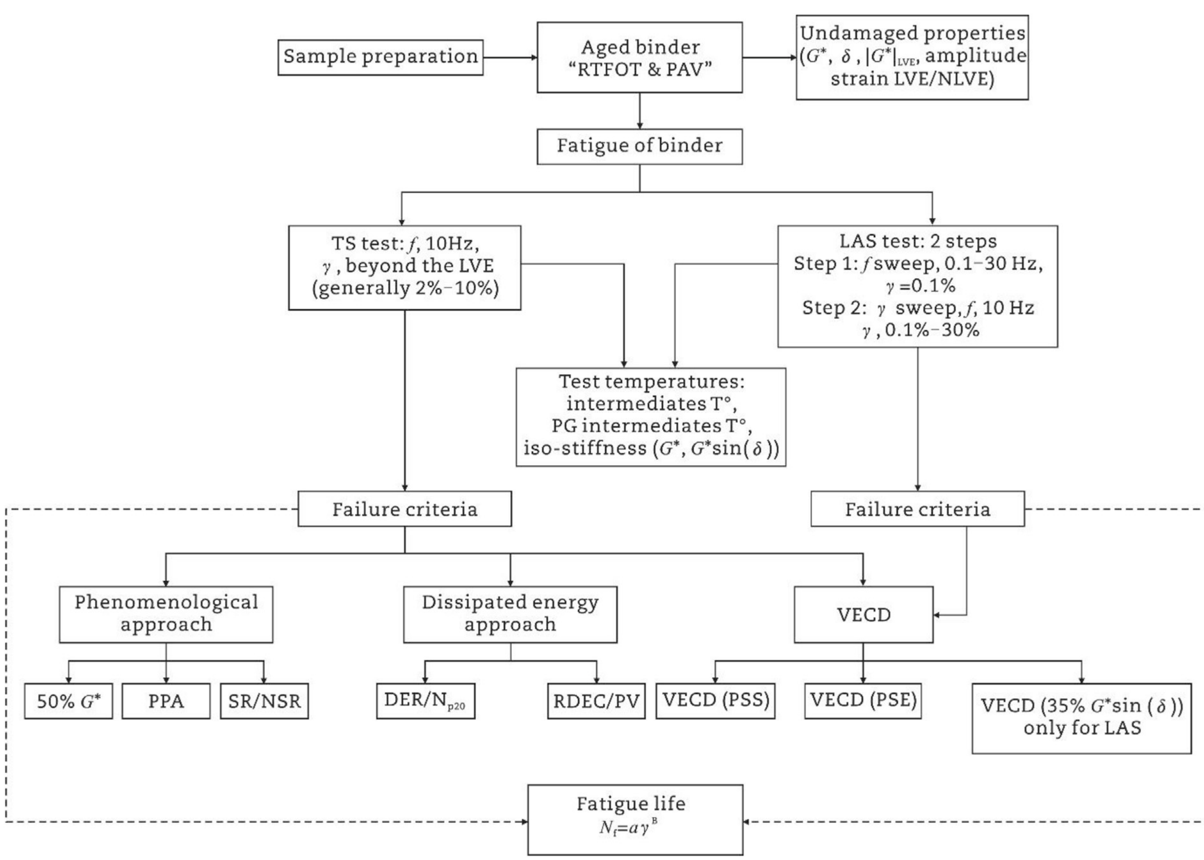

Fig. 5 – Flowchart of evaluation of fatigue life of asphalt binder using the TS and LAS tests.

test (BYET) for characterizing the fatigue life of asphalt binders using the DSR (8 mm parallel plates with 2 mm gap). The BYET is conducted under constant strain rate loading, resulting in linearly increasing shear strain over time, thereby causing the binder to accumulate damage more rapidly compared to the TS test. The BYET is performed according to AASHTO TP 123-16 (AASHTO, 2016) at a selected temperature by the application of a constant shear rate of 2.3% s^{-1} for 30 min. During the test, stress and strain are measured, allowing the construction of a stress-strain curve. This curve depicts shear stress increasing with shear strain until peak shear stress is reached, after which it decreases. The yield energy, defined as the area under the stress-strain curve up to the peak shear stress (as illustrated in Fig. 6), and the shear strain, corresponding to the peak shear stress ($\gamma_{\tau max}$), are measured at the end of the test. These parameters serve as indicators for fatigue resistance (Johnson et al., 2009). However, O'Connell et al. (2017) observed a poor correlation between the fatigue life of South African binders assessed using the BYET test and that of asphalt mixtures evaluated through the four-point bending beam fatigue test. Consequently, they did not recommend utilizing the BEYT to predict the fatigue life of asphalt binders in South Africa.

As the BYET is only an indicator for fatigue, it is not largely used to evaluate the fatigue life of asphalt binder. In 2010, Johnson and Bahia (2010) introduced the linear amplitude sweep test (LAS) based on viscoelastic continuum damage (VECD) concepts (section 4). The LAS test is recognized as an accelerated procedure for characterizing the fatigue life of asphalt binders. Similar to the TS and BYET tests, the LAS test is conducted using a DSR (8 mm parallel plates with 2 mm gap) under increased loading amplitudes. The LAS test comprises two steps: the frequency sweep followed by the strain amplitude sweep. The frequency sweep aims to define the undamaged properties and the α parameter defined in section 4. During the frequency sweep, the amplitude strain is maintained constant at 0.1% (within the LVE range), while the frequency ranges from 0.1 to 30 Hz. Subsequently, the amplitude sweep test can be performed immediately after the frequency sweep, maintaining a frequency of 10 Hz and employing amplitude strains ranging from 0.1% to 30.0%. Each strain level undergoes 100 cycles over 10 s, resulting in a total duration of 310 s and 3100 cycles in a full loading

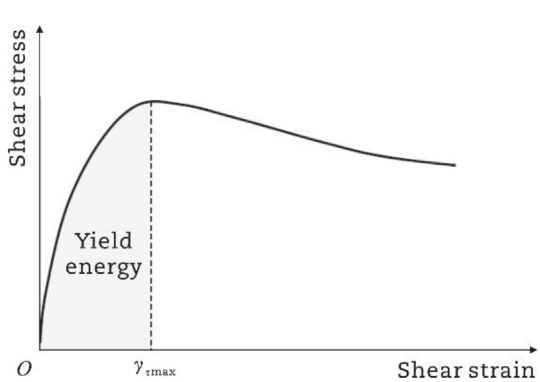

Fig. 6 – Yield energy from BYET test (Johnson et al., 2009; Zeiada et al., 2022).

cycle (as depicted in Fig. 7(a)) (AASHTO, 2021; Johnson, 2010; Johnson and Bahia, 2010).

The LAS test is typically conducted at intermediate temperatures. For some types of rheometers incapable of instantaneously applying a 1% increase in loading amplitude between two intervals, Hintz and Bahia (2013) proposed a modified LAS test, increasing the loading amplitude by 0.1% per second up to 30% (Fig. 7(b)). This modification, which maintains the frequency constant, ensures that the total duration and loading cycles remain unchanged compared to the original LAS test. This modified LAS test is standardized in AASHTO TP 101-14 (AASHTO, 2014). While LAS standards do not specify the number of replicates, Hintz et al. (2011) suggested that the difference between two replicates should be less than 15%; otherwise, a third test is recommended.

In summary, the time sweep (TS), linear amplitude sweep (LAS), and binder yield energy test (BYET) should all be conducted on RTFOT or PAV-aged asphalt binders. Since 2017, the LAS test has emerged as the most widely used fatigue test for evaluating the fatigue life of asphalt binders, as depicted in Fig. 8. Conversely, the BYET is the least utilized test for evaluating the fatigue life of asphalt binders compared to the TS and LAS tests.

3. Fatigue failure criteria and fatigue failure definition

In some papers, there is a real confusion between the fatigue failure criterion and fatigue failure definition. The fatigue failure criterion refers to the law governing the material behavior during damage, either through a mechanistic or empirical approach, while the fatigue failure definition is the identification of the fatigue failure point (fatigue life) of asphalt materials. According to Zhang et al. (2013), the failure criterion defines the applicable region associated with the continuum damage model and is important in characterizing the fatigue failure point (service life) of asphalt materials.

In the literature, various fatigue failure criteria and failure definitions are utilized to predict the fatigue life of both asphalt mixtures and binders. As previously mentioned, failure criteria are typically divided into two main groups, phenomenological failure criteria and dissipated energy-based failure criteria. Initially the fatigue failure criteria and failure definitions have been developed to evaluate the fatigue life of asphalt mixtures, they are now commonly employed to predict the fatigue life of asphalt binders as well.

3.1. *Phenomenological failure criteria*

This approach is based on the variation of stiffness modulus and phase angle with loading cycles to define the fatigue life of asphalt mixtures and asphalt binders. Raithby and Sterling (1972) were the first researchers to define fatigue life as the loading cycles corresponding to a 50% reduction in the initial stiffness modulus, referred to as $N_{f50\%}$. Because of its simplicity, the 50% reduction in the stiffness modulus compared to the undamaged modulus is still used. Despite its simplicity, this failure definition has been largely

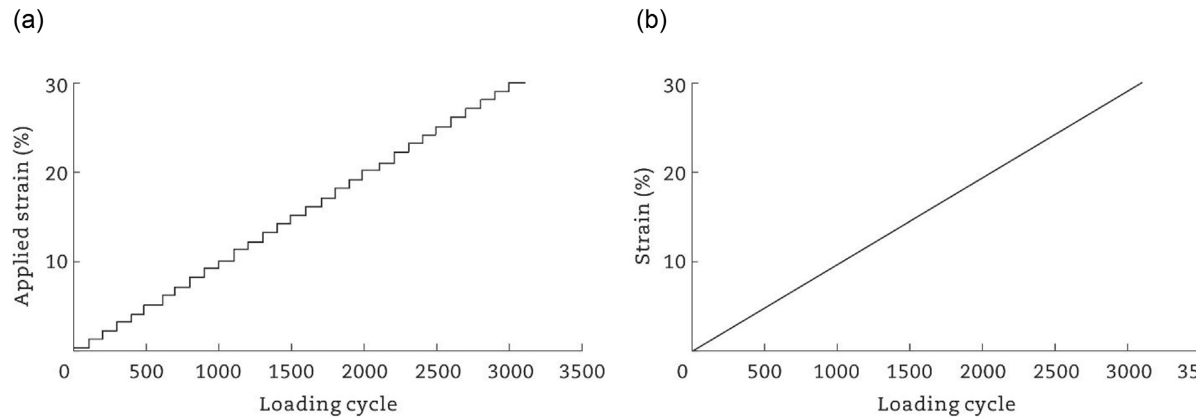

Fig. 7 – Typical loading scheme for LAS test. (a) According to AASHTO T 391-20 (AASHTO, 2021). (b) According to AASHTO TP 101-14 (AASHTO, 2014).

criticized in literature; some researchers consider that this failure definition lacks solid theoretical support (Zeiada et al., 2022; Zhang et al., 2013). Furthermore, studies by Zhang et al. (2013) and Basueny et al. (2015) have shown that the fatigue life at 50% reduction in stiffness modulus, $N_{f50\%}$, of asphalt mixture is often far from the failure point (Fig. 9(a)). In response to these limitations, Reese (1997) proposed an alternative approach to defining fatigue life, as the loading cycles corresponding to the phase angle peak (Fig. 9(b)). During fatigue testing, the phase angle typically increases linearly with the loading cycles before sharply decreasing. Reese (1997) identified this sharp decrease as the point of fatigue failure. According to Zhang et al. (2013), the abrupt modification of the phase angle indicates a significant transformation occurring within the material. Consequently, Reese's approach is considered more consistent compared to the 50% stiffness reduction.

Rowe and Bouldin (2000) introduced a new phenomenological fatigue failure criterion known as the stiffness ratio (SR), which is based on the energy ratio (Eq. (9)) described in subsection 3.2. The SR is applicable in both controlled-stress (Eq. (1)) and controlled-strain modes (Eq. (2)), where the ratio of $\sin(\delta_0)/\sin(\delta_i)$ is assumed to be 1. Adhikari et al. (2009) further extended this concept and proposed the normalized rowe and bouldin stiffness ratio (NSR) (Eq. (3)).

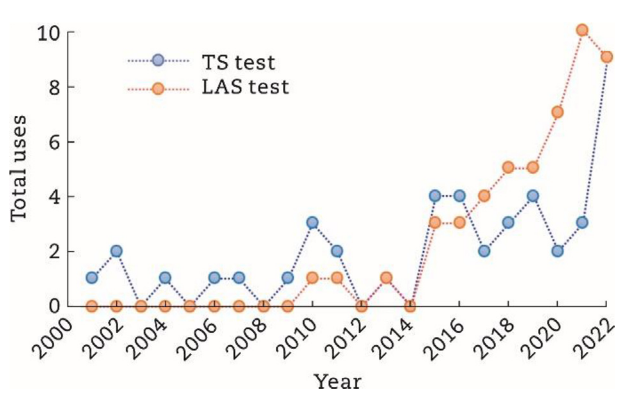

Fig. 8 – Evolution of the utilization of the TS and LAS test in literature (from the 81 reviewed papers).

$$SR^{\sigma} = i\,|G_i^*| \tag{1}$$

$$SR^{\epsilon} = \frac{i}{|G_i^*|} \tag{2}$$

$$NSR = \frac{i\,|G_i^*|}{|G_0^*|} \tag{3}$$

where i is the load cycle number, G_i* is the complex modulus at load cycle i and G_0* is the initial undamaged complex modulus, taken at cycle number of 50 according to Adhikari et al. (2009). They do not explain the reason to take the initial undamaged complex modulus at cycle number of 50.

For both SR and NSR methods, the fatigue life is defined as the number of cycles corresponding to the peak of SR and NSR curves, as illustrated in Fig. 10.

Some researchers have argued that phenomenological failure criteria may not effectively account for viscoelastic effects and therefore cannot reliably predict the fatigue life of asphalt binders (Sun et al., 2019; Yue et al., 2021). Shen et al. (2006) pointed out limitations of phenomenological failure criteria, including their inability to consider damage evolution and their dependence on loading conditions (controlled stress or strain), test methods, and material types. Moreover, the phenomenological failure criteria presents a severe difficulty in investigating the healing phenomenon and the fatigue endurance limit (Shen et al., 2006). To address these limitations, alternative criteria based on the dissipated energy approach have been developed.

It is worth noting that the three failure criteria mentioned above are employed to predict the fatigue life of asphalt binders in the TS test. However, these criteria are not applicable in the LAS test due to the continuous increases in applied loading. Among the 81 reviewed research papers, 17 research papers utilized the phenomenological approach to evaluate the fatigue life of asphalt binders using the TS test. The 50% reduction in G* failure definition was employed in 13 research papers; while the peak phase angle and peak in SR and NSR failure definitions were used in 6 and 5 research papers, respectively.

Some researchers employed two or three failure definitions within the same paper, as indicated in Table 2. The traditional

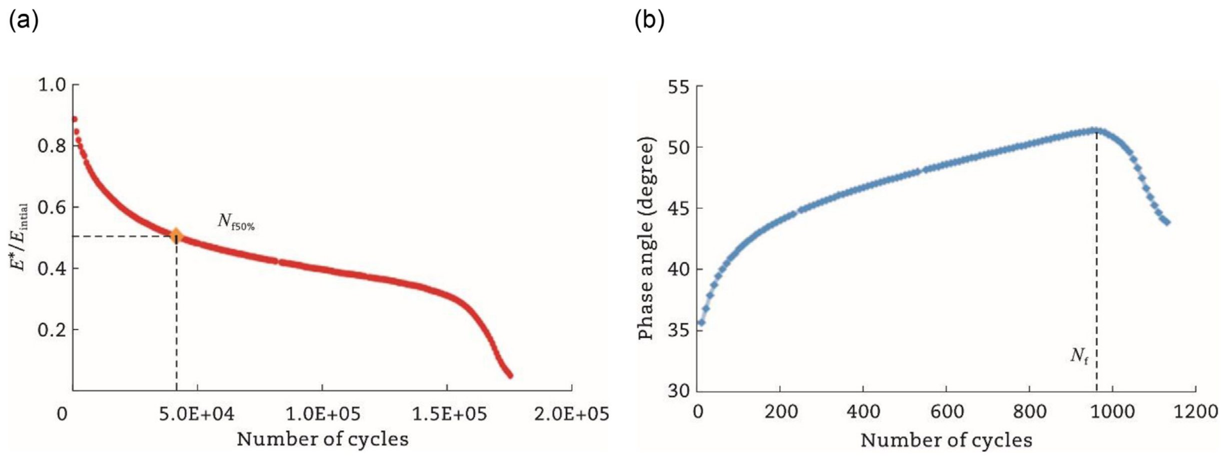

Fig. 9 – Fatigue life of asphalt mixture. (a) 50% stiffness reduction. (b) Peak of phase angle (Zhang et al., 2013).

failure definition (50% reduction in stiffness) remains the most commonly used. The main conclusions on these failure definitions are given in section 5.

3.2. *Dissipated energy-based failure criteria*

The dissipated energy in a viscoelastic material, which represents the energy loss through mechanical work, heat release, or damage, is quantified by calculating the area under the stress-strain curve (Eq. (4)) (Ghuzlan and Carpenter, 2006; Hintz, 2012; Johnson, 2010).

$$W_i = \pi\, \sigma_i\, \epsilon_i\, \sin(\delta_i) \tag{4}$$

where W_i is the dissipated energy, σ_i is the stress amplitude, ϵ_i is the strain amplitude, and δ_i is the phase angle at the cycle load *i*. In controlled strain mode, the dissipated energy can be calculated using Eq. (5), while in controlled stress mode, Eq. (6) is employed (Rowe and Bouldin, 2000; Zeiada et al., 2022).

$$W_i = \pi\, \epsilon^2 G_i^*\, \sin(\delta_i) \tag{5}$$

$$W_i = \pi\, \frac{\sigma^2}{G_i^*} \sin(\delta_i) \tag{6}$$

where G_i^* is the complex modulus at load cycle *i*.

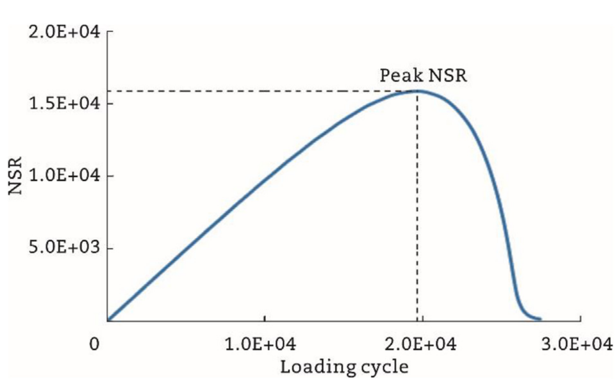

Fig. 10 – Fatigue life based on normalized stiffness ratio method (Zeiada et al., 2022).

The total dissipated energy W is given in Eq. (7).

$$W = \sum_{i=1}^{n} W_i \tag{7}$$

Van Dijk et al. (1972) were the first researchers who proposed a relationship between fatigue life (N_f) of asphalt mixtures and the total dissipated energy (*W*), assuming that all dissipated energy contributes to damage. This relationship is represented by Eq. (8).

$$W = A\, N_f^{\,B} \tag{8}$$

where *A* and *B* are material constants.

As a consequence of Van Dijk et al. (1972) pioneering work, three primary failure criteria based on dissipated energy were developed.

- The energy ratio (ER), proposed by Hopman et al. (1989), represented by Eq. (9).
- The dissipated energy ratio (DER) or, in some papers, the cumulative dissipated energy (CDER), proposed by Pronk and Hopman (1991), expressed by Eq. (10).
- The ratio of dissipated energy change (RDEC), developed by Ghuzlan and Carpenter (2000), represented by Eq. (11).

$$ER = \frac{i\, W_0}{W_i} \tag{9}$$

$$DER = CDER = \frac{\sum_{i=1}^{n} W_i}{W_n} \tag{10}$$

$$RDEC = \frac{W_{i+1} - W_i}{W_i} \tag{11}$$

where W_i and W_{i+1} are the dissipated energy at cycle *i* and *i*+1 respectively.

The fatigue life is predicted directly from the variation of DER and RDEC with the loading cycle. As for the DER, the fatigue life is defined by Bahia et al. (2001) and Bonnetti et al. (2002) as the number of cycles to reach the crack propagation stage, N_p, based on the intersection of the two

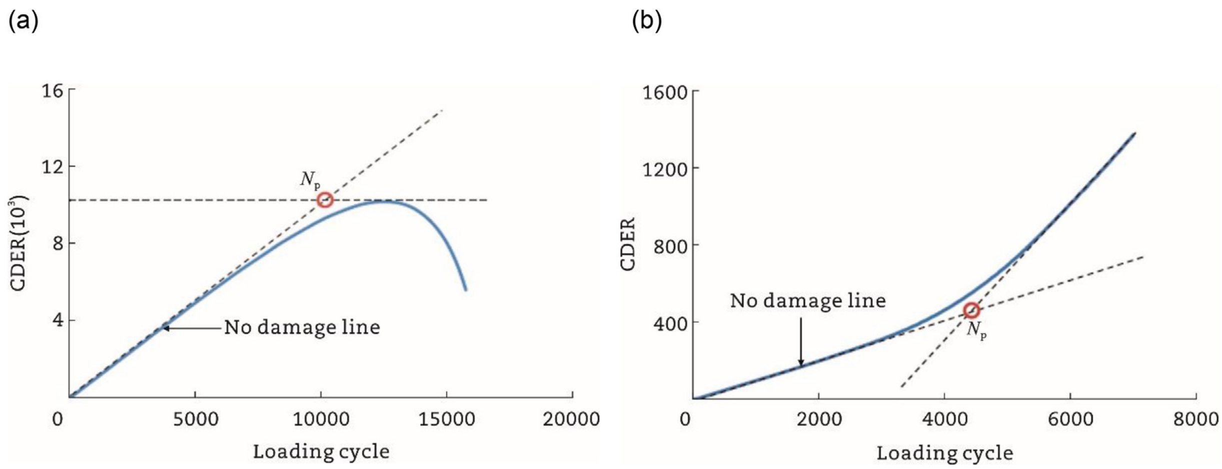

Fig. 11 – Fatigue life based on crack propagation (Zeiada et al., 2022). (a) Stress-controlled test. (b) Strain-controlled test.

tangent lines (Fig. 11). It can be observed that the N_p depends on the loading mode. In the case of a stress-controlled test, the increase of loading cycle increases the phase angle and strain amplitude and decreases the stiffness due to the accumulation of damage (Hajj and Bhasin, 2018). Consequently, the dissipated energy increases with the loading cycle, while the DER increases linearly with loading cycles until it reaches a maximum value (failure) and then drops brutally when the material fails (Fig. 11(a)). In the case of a strain-controlled test, the material weakens during the test and presents lower stress resistance. Consequently, the dissipated energy reduces, and the DER steadily increases (Fig. 11(b)). Because of that, the failure point is unclear (Bonnetti et al., 2002).

In order to establish a unified failure definition irrespective of the loading mode (stress or strain-controlled test), Bonnetti et al. (2002) introduced the N_{p20} parameter. N_{p20} represents the loading cycle corresponding to a 20% deviation of the dissipated energy ratio (DER) curve from the no-damage line. While the DER concept assumes that all dissipated energy contributes to damage, this assumption is criticized by Ghuzlan and Carpenter (2000). They argue that only a portion of dissipated energy drives damage, considering the viscoelastic effect. Therefore, Ghuzlan and Carpenter (2000) proposed using the variation of ratio of dissipated energy change (RDEC) with load cycles (N) to define the fatigue life (N_f) of asphalt mixtures. The RDEC vs. N curve (Fig. 12) can be categorized into three stages. The first stage corresponds to decreasing of RDEC with load cycles. The second stage corresponds to practically no variation of RDEC with load cycles, defined as plateau value (PV) by Ghuzlan and Carpenter (2000). While the third stage corresponds to a rapid increase in the RDEC values (Fig. 12). The fatigue failure is defined as the loading cycle corresponding to the transition point between the PV and the third stage. Shen et al. (2006) applied the RDEC approach to define the fatigue life of asphalt binders and mastics, finding a strong relationship between PV and $N_{f50\%}$ curves for asphalt binders and asphalt mixtures. Similarly, Pereira et al. (2016) observed the same relationship (Fig. 13), defining the PV as the RDEC value corresponding to a 50% reduction in stiffness.

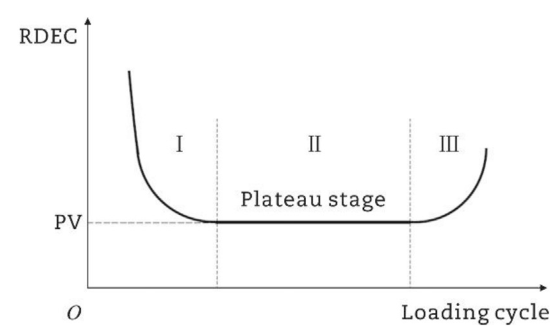

Fig. 12 – Variation of RDEC with load cycles (Zeiada et al., 2022).

Due to the nature of continuous increases in applied loading in the LAS test, dissipated energy-based failure criteria are primarily utilized to predict the fatigue life of asphalt binders in the TS test. As indicated in Table 2, among the 81 reviewed papers, 22 research papers employed the DER/N_{p20} and RDEC approaches to investigate the fatigue life of asphalt binders using the TS test. Specifically, 7 research papers utilized both the DER/N_{p20} and RDEC approaches as failure definitions, 11 papers exclusively used the DER/N_{p20} failure definition, and 5 research papers relied on the RDEC approach. Notably, the DER approach emerged as the most commonly used dissipated energy-based failure criterion.

Establishing the relationship between fatigue life (N_f) and load amplitude (γ) of asphalt mixtures and binders using dissipated energy-based failure criteria necessitates conducting several tests at different applied amplitudes. However, this time-consuming procedure has prompted researchers to adopt viscoelastic continuum damage (VECD) mechanics to predict the fatigue life of asphalt mixtures and binders at different load amplitudes from a single test (Hintz, 2012). VECD is primarily employed in the LAS test to examine damage evolution and the fatigue life of asphalt binders.

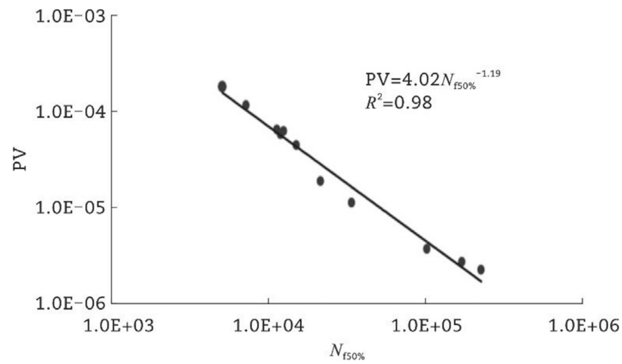

Fig. 13 – Relationship between PV and $N_{f50\%}$ (Pereira et al., 2016).

4. Viscoelastic continuum damage (VECD) approach

The mechanistic VECD model is extensively utilized for predicting damage progression and fatigue life in viscoelastic materials. This approach focuses on macroscopic behavior, quantifying effective stiffness and damage as loading continues. The effective stiffness, measured experimentally, is defined as the material's integrity. The damage (D), or the internal state variable (S) in some papers, is quantified empirically based on Schapery's theory. Schapery (1990) developed the work potential theory for elastic materials with growing damage. The damage evolution law for elastic material is given in Eq. (12).

$$\frac{dD}{dt}=\left(-\frac{\partial W}{\partial D}\right)^{\alpha} \tag{12}$$

where α is the damage evolution rate, and W is the total dissipated energy (strain energy density in some papers).

The damage evolution law of elastic materials was extended to viscoelastic materials (asphalt mixtures) by Park et al. (1996) (Eq. (13)) in which the physical strain ϵ is transformed to pseudo strain ϵ^R. The introduction of pseudo strain aims to eliminate the time effects of viscoelastic materials. Based on the elastic-viscoelastic correspondence principle, Schapery (1984) defined the pseudo strain ϵ^R as shown in Eq. (14). Therefore, the form of Eq. (14) is identical to Hooke's law for elastic materials.

$$\frac{dD}{dt}=\left(-\frac{\partial W^R}{\partial D}\right)^{\alpha} \tag{13}$$

$$\epsilon^R=\frac{1}{E_R}\sigma \tag{14}$$

where E_R is the reference modulus, typically taken as one. Thus, in the linear viscoelastic domain (LVE), the pseudo strain equals the LVE shear stress. Then, Eq. (14) can be rewritten as indicated in Eq. (15), where $|G^*|_{LVE}$ is the linear viscoelastic complex shear modulus.

$$\epsilon_i^R=\epsilon_i\,|G^*|_{LVE} \tag{15}$$

The damage evolution rate related to the material's creep or relaxation properties, α, is determined from the slope m of the log-log plot of relaxation or creep with time. According to Lee and Kim (1998), $\alpha=1+\frac{1}{m}$ for strain-controlled tests and $\alpha=\frac{1}{m}$ for stress-controlled tests.

And W^R is the pseudo-strain energy density, defined in Eq. (16).

$$W^R=\frac{1}{2}\left(\epsilon^R\right)^2 C \tag{16}$$

where C is the material integrity (or pseudo-stiffness) defined in Eq. (17).

$$C=\frac{\sigma_P}{\epsilon_p^R\,\text{DMR}} \tag{17}$$

where ϵ_p^R is the peak pseudo-strain, σ_P is the peak shear stress, and DMR (dynamic modulus ratio) is the specimen-to-specimen variability factor, given in Eq. (18). Where $|G^*|_{initial}$ is the undamaged complex shear modulus. The DMR value range from 0.9 to 1.1 (Cao and Wang, 2018; Yue et al., 2021).

$$\text{DMR}=\frac{|G^*|_{initial}}{|G^*|_{LVE}} \tag{18}$$

From Eqs. (15), (17) and (18), the material integrity can be simplified as indicated in Eq. (19).

$$C(t)=\frac{|G^*|_t}{|G^*|_{initial}} \tag{19}$$

The relationship between $C(t)$ and $D(t)$ is given in Eq. (20) (Kim et al., 2006). It is assumed that at $t=0$, $C=C_0=1$ (undamaged material) and $D=0$ (AASHTO, 2014; Kim et al., 2006).

$$C(t)=C_0-C_1\,D^{C_2} \tag{20}$$

C_1 and C_2 can be derived from Eq. (21).

$$\log(C_0-C(t))=\log C_1+C_2\log D(t) \tag{21}$$

The damage accumulation as a function of time is given in Eq. (22).

$$D(t)=\sum_{i=1}^{n}\left[\frac{\text{DMR}}{2}\left(\epsilon_p^R\right)^2(C_{i-1}-C_i)\right]^{\frac{\alpha}{\alpha+1}}(t_i-t_{i-1})^{\frac{1}{1+\alpha}} \tag{22}$$

According to Kim et al. (2006), the damage at failure, D_f, corresponds to the peak shear stress (Fig. 14) and can be

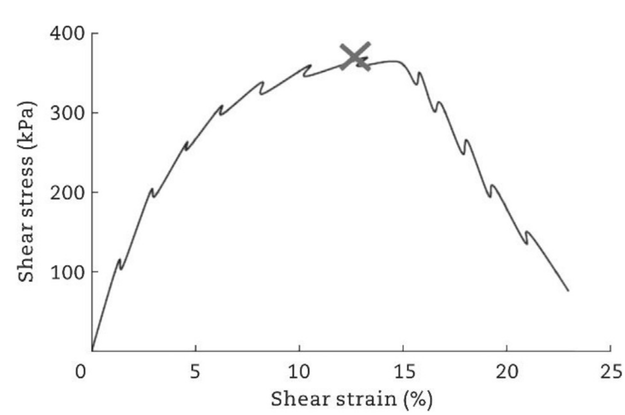

Fig. 14 – Stress-strain curve from the LAS test (Roque et al., 2020).

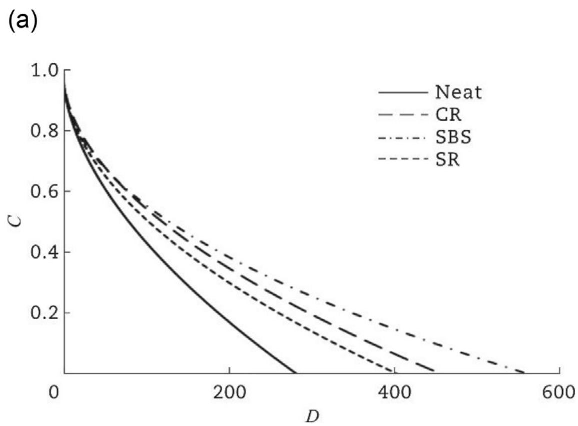

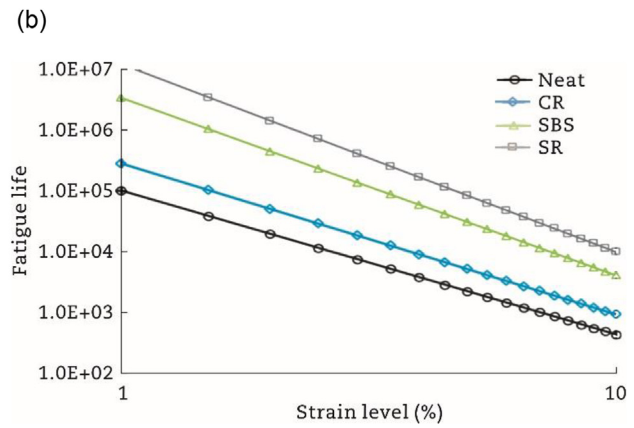

Fig. 15 – Damage characteristics curve C(D) and the fatigue life curve (Zhang et al., 2020). (a) Typical damage characteristic curve C(D). (b) Typical fatigue life curve from LAS test (CR means crumb rubber, SR means SBS+CR).

determined using Eq. (23). It is referred as peak shear stress (PSS) failure definition.

$$D_f = \left(\frac{C_0 - C_{\text{at peak stress}}}{C_1}\right)^{\frac{1}{C_2}} \tag{23}$$

The fatigue life parameters A and B (Eq. (24)) can be calculated following Eqs. (25) and (26), respectively.

$$N_f = A\gamma^{-B} \tag{24}$$

$$A = \frac{f\ (D_f)^k}{k(\pi\ C_1 C_2)^{\alpha}} \tag{25}$$

where $k = 1 + (1 - C_2)\alpha$ and f is the frequency, $f = 10$ Hz.

$$B = 2\alpha \tag{26}$$

The higher the value of A, the longer the fatigue life. Meanwhile at a constant A, the higher the value of B, the shorter the fatigue life. Based on the VECD, the damage characteristic curve $C(D)$ and the fatigue life curve can then be plotted. Fig. 15(a) and (b) show, respectively, the typical damage characteristic curve and the typical fatigue life curve of some binders (neat and modified with different additives).

The VECD concept developed by Kim et al. (2006) was widely utilized in the literature to predict the fatigue life of asphalt binder using both the TS and LAS tests (Bessa et al., 2019; Błażejowski et al., 2020; Kavussi and Barghabany, 2016; Kuchiishi et al., 2019; Mirhosseini et al., 2017; Morshed et al., 2020; Sun et al., 2019). In 2010, Johnson (2010) applied the VECD to define the fatigue life of asphalt binders using the LAS test. However, Johnson employed the dissipated strain energy density W (Eq. (4)) to quantify the work performed (Eq. (27)), whereas Kim et al. (2006) utilized the pseudo strain energy density.

$$\frac{dD}{dt} = \left(-\frac{\partial W}{\partial D}\right)^{\alpha} \tag{27}$$

So, Johnson (2010) defined the damage accumulation for asphalt binder as given in Eq. (28).

$$D(t) = \sum_{i=1}^{n}\left[\pi I_D\ \gamma^2(|G^*|\sin(\delta_{i-1}) - |G^*|\sin(\delta_i))\right]^{\frac{\alpha}{\alpha+1}}(t_i - t_{i-1})^{\frac{1}{1+\alpha}} \tag{28}$$

where I_D is the initial undamaged $|G^*|$, δ is the phase angle, and γ is the applied shear strain amplitude.

In Johnson's approach (Johnson, 2010), $|G^*|\sin(\delta)$ represents the material integrity C, and the α parameter is calculated using the slope m of the log $G'(\omega)$ versus $\log(\omega)$ plot, based on the inter-conversions between the relaxation modulus $G(t)$ and the storage modulus $G'(\omega)$ proposed by Schapery and Park (1999).

The power law equation related the material integrity with damage becomes (Eq. (29)).

$$|G^*|\sin(\delta) = C_0 - C_1 D^{C_2} \tag{29}$$

where C_0 is the initial undamaged $|G^*|\sin(\delta)$.

Some researchers (Li et al., 2022; Zhang et al., 2020, 2022) used the normalized $|G^*|\sin(\delta)$ to define the material integrity C (Eq. (30)); therefore, $C_0 = 1$ (undamaged material).

$$C_i = \frac{|G_i^*|\sin(\delta_i)}{|G_0^*|\sin(\delta_0)} \tag{30}$$

According to Johnson (2010), the damage at failure, D_f, corresponds to the 35% reduction in $|G^*|\sin(\delta)$, it can be determined using the following Eq. (31). Johnson (2010) found a good correlation between the fatigue life evaluated based on the N_{p20} parameter using the TS test and the 35% reduction in $|G^*|\sin(\delta)$ using the LAS test. Consequently, the 35% reduction in $G^*\sin(\delta)$ failure definition has been adopted in the LAS specification according to AASHTO T 391-20.

$$D_f = 0.35\left(\frac{C_0}{C_1}\right)^{\frac{1}{C_2}} \tag{31}$$

Aurilio et al. (2021), Li et al. (2022) and Mannan et al. (2015) defined the damage at failure D_E as the 50% reduction of the normalized $|G^*|\sin(\delta)$ (Eq. (32)), to link with the $N_{f50\%}$ used for asphalt mixes.

$$D_f = 0.5\left(\frac{C_0}{C_1}\right)^{\frac{1}{C_2}} \tag{32}$$

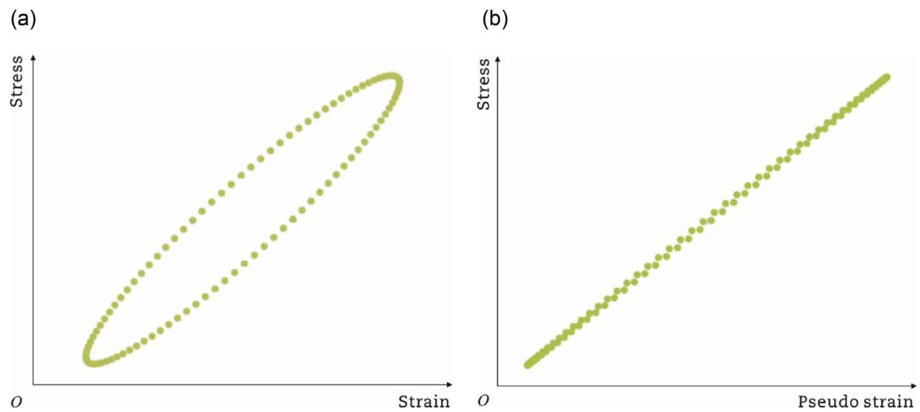

Fig. 16 – Viscoelasticity effect for undamaged material (Zhang et al., 2013). (a) Dissipated strain energy. (b) Dissipated pseudo strain energy.

In Johnson's approach (Johnson, 2010), the fatigue life parameter A is calculated according to Eq. (33). While the parameter B remains unchanged compared to that of Kim et al. (2006) (Eq. (23)).

$$A=\frac{f\ (D_f)^k}{k(\pi\ I_D\ C_1C_2)^\alpha} \tag{33}$$

Johnson's approach (Johnson, 2010) has been standardized in the current specification of the LAS test (AASHTO, 2021). In Johnson's approach (Johnson, 2010), based on the dissipated strain energy, it is assumed that the total dissipated strain energy does damage. However, the dissipated strain energy also includes the energy associated to viscoelastic damping (viscous dissipation) (Cao and Wang, 2018). In effect, only a portion of the dissipated strain energy is responsible for damage growth. However, in the dissipated pseudo-strain energy approach, the elastic-viscoelastic correspondence principle eliminates the effect of viscoelasticity. Consequently, Cao and Wang (2018) recommended the utilization of the VECD approach founded on the pseudo-strain energy proposed initially by Park et al. (1996), based on the elastic-viscoelastic correspondence principle.

As indicated above, the dissipated strain energy W (Eq. (4)) is the area inside the loop of the stress-strain curve (Fig. 16(a)). The area of the dissipated pseudo strain energy W^R can be calculated using Eq. (34).

$$W_i^R=\pi\ \sigma_i\epsilon_i^R\ \sin\ (\delta_i-\delta) \tag{34}$$

where δ_i is the phase angle at cycle i, δ is the undamaged phase angle measured in the LVE domain due to the viscoelasticity of the material. When the material is undamaged, the δ_i is approximately equal to the initial δ. Therefore, the dissipated pseudo strain energy tends to zero, and the pseudo hysteresis loop converges into a line (Fig. 16(b)). However, when the applied load exceeds the endurance limit, the material undergoes damage, and the pseudo hysteresis increases due to the increase of phase angle δ_i, while δ (viscoelasticity effect) remains constant. Consequently, the pseudo hysteresis transforms from a line (undamaged material) into an elliptical shape (damaged material), as indicated in Fig. 17. As the viscoelasticity effect has been removed using the pseudo strain energy, the change in the pseudo strain energy is due principally to damage unlike the dissipated energy in which the change is due to the combined viscoelasticity and damage effect.

Similarly, Wang et al. (2015), proposed the pseudo-strain energy (PSE) based method to define the failure of asphalt binder using the LAS test. The total PSE, termed as W^R_{Total} (Eq. (35)), is the sum of cumulative released PSE W^R_r (Eq. (36)) and cumulative stored PSE W^R_s (Eq. (37)). Fig. 18 shows the stress-pseudo strain curve obtained from the LAS test (Wang et al., 2015). The total PSE injected into the material by the applied load, represents the area under the undamaged line, the released PSE by the material due to damage represents the area between the undamaged and damaged line (area with red lines), and the stored PSE represents the area under the damaged line (area with black lines). This pseudo-strain energy (PSE) concept is used initially on the asphalt mixtures by Zhang et al. (2013).

$$W^R_{Total}=\frac{1}{2}\ (\epsilon^R)^2 \tag{35}$$

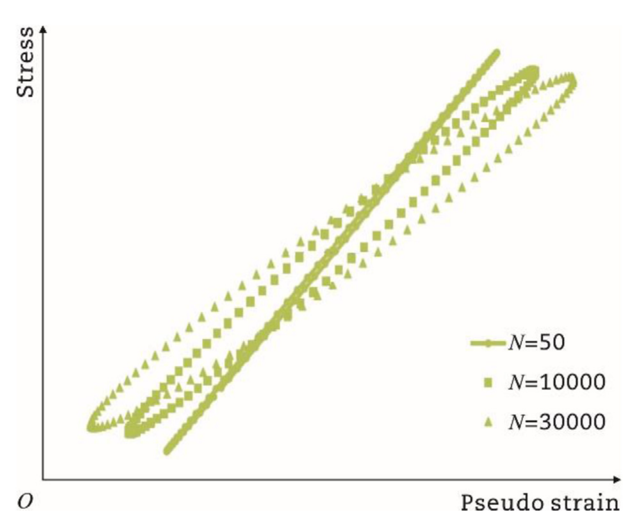

Fig. 17 – Psseudo hysterisis loop for damaged material (Zhang et al., 2013).

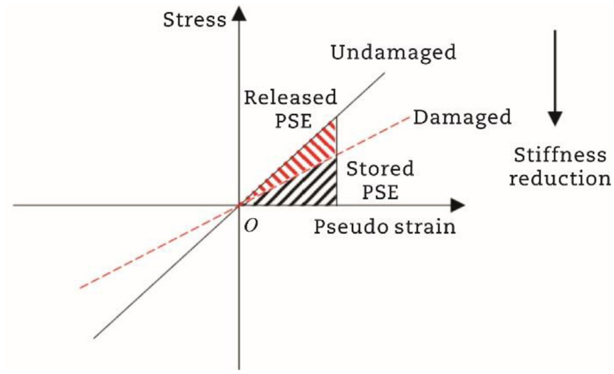

Fig. 18 – Total, released, and stored PSE in stress-pseudo strain curve (Roque et al., 2020; Wang et al., 2015).

$$W_s^R = \frac{1}{2}\, C\, (\epsilon^R)^2 \tag{36}$$

$$W_r^R = \frac{1}{2}\, (1 - C)\, (\epsilon^R)^2 \tag{37}$$

where C is the material integrity (defined above in Eq. (17)). $C = 1$ when the material presents a linear viscoelastic behavior and decreases when the material undergoes damage.

The number of cycles corresponding to the maximum stored PSE is defined, by Wang et al. (2015), as the fatigue life (N_f) of asphalt binder (Fig. 19).

Wang et al. (2015) observed a good correlation between the fatigue life (N_f) obtained from the LAS test using the maximum stored PSE failure definition and that obtained from the TS test using the peak phase angle failure definition with an R^2 value of 0.99.

In their study, Zhang et al. (2013) illustrated the evolution of the total released PSE of asphalt mixtures (Fig. 20). They noted that the rate of the total released PSE, termed as G^R, remains almost constant. Initially, G^R is used to represent the steady rate of damage accumulation. However, Sabouri and Kim (2014) redefined the G^R parameter as the rate of change of the averaged released PSE ($\overline{W_r^R}$) as indicated in Eq. (38), where A_r is the area of released PSE before reaching the fatigue life (Fig. 19). They demonstrated that the relationship between fatigue life and the average G^R is independent of loading history, loading mode and temperature.

$$G^R = \frac{\overline{W_r^R}}{N_f} = \frac{\int_0^{N_f} W_r^R}{{N_f}^2} = \frac{A_r}{{N_f}^2} \tag{38}$$

In 2015, Wang et al. (2015) introduced the G^R approach to develop the simplified viscoelastic continuum damage (S-VECD) model of asphalt binders for analyzing the results of the LAS test. They demonstrated that the relationship between the G^R parameter and the fatigue life N_f can be expressed as shown in Eq. (36) (Fig. 21). Additionally, they illustrated that the G^R approach is unaffected by loading history and temperature. This relationship (Eq. (39)) is established by conducting LAS tests at various constant strain-amplitude rates (CSR), as outlined in subsection 7.3.

$$G^R = a{N_f}^b \tag{39}$$

where a and b are the failure criterion model constants.

Based on the G^R failure criterion, the improved fatigue life formula is given in Eq. (40).

$$N_f = \left[\frac{K}{a}\, \gamma^{2+2\alpha\left(\frac{C_2}{p}\right)}\right]^{\frac{1}{b+1-\frac{C_2}{p}}} \tag{40}$$

where

$$p = 1 - \alpha C_2 + \alpha$$

$$q = \frac{2^\alpha f}{(1 - \alpha C_2 + \alpha)(C_1\, C_2)^\alpha\, (|G^*|_{LVE})^{2\alpha}}$$

$$K = \frac{1}{2}\, C_1\, (|G^*|_{LVE})^2\, q^{-\frac{C_2}{p}}\, \frac{1}{\frac{C_2}{p} + 1}$$

To summarize, the utilization of the VECD approach varies significantly depending on whether pseudo strain energy, dissipation energy, or the G^R approach is employed, as outlined in Table 1. As indicated in Table 2, the VECD approach is predominantly utilized for analyzing the results of the LAS test. Only three research papers (Baglieri et al., 2018; Safaei and Castorena, 2020; Underwood, 2016) employed the S-VECD (PSE) to predict the fatigue life of asphalt binders using the TS test. It can be seen from Table 2 that the S-VECD (PSE) is the most commonly used failure definition, appearing in 26 papers, followed by the VECD (PSS) with 16 uses, and finally the VECD (35% reduction in $G^*\sin(\delta)$) which is used in 15 papers. Some papers incorporate two or three failure definitions, as displayed in Table 2. It is worth noting that among the 81 research papers reviewed on the fatigue life of asphalt binders using the TS, BYET and LAS test, 68 of them employed the fatigue life failure definitions mentioned above (Table 2); the remaining papers utilized other indices or methods to interpret the fatigue test results.

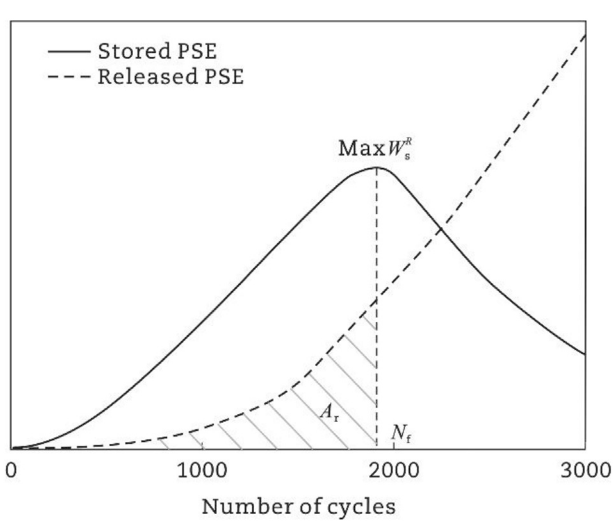

Fig. 19 – Fatigue life (N_f) using maximum stored PSE (Yue et al., 2021).

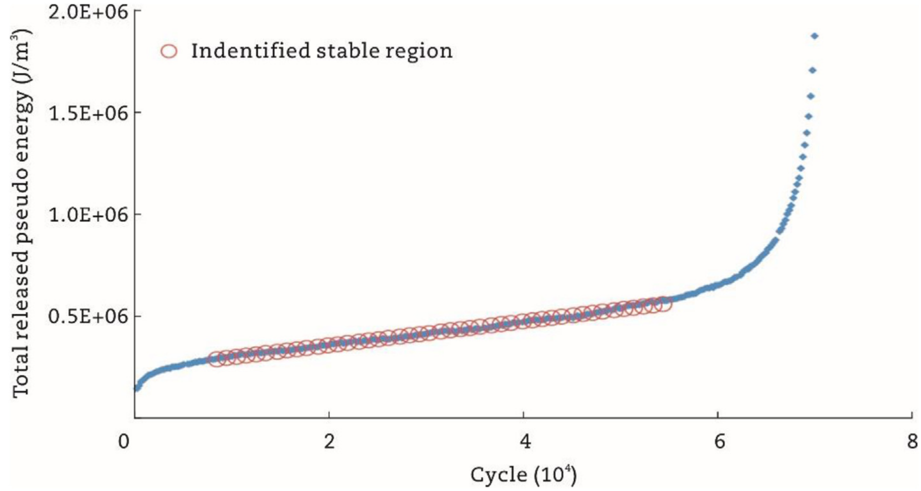

Fig. 20 – Evolution of total released PSE with cycle load (Zhang et al., 2013).

5. Correlation between different failure definitions used in the TS and LAS tests

As mentioned above, the fatigue life of asphalt mixtures and asphalt binders depends strongly on the used failure criterion and the definition of failure point. Several failure criteria and failure definitions have been proposed and tested to predict asphalt materials' fatigue life (sections 3 and 4). This section reviews the correlations and relationships between the different failure criteria and failure definitions used to evaluate the fatigue life of asphalt binders using the time sweep and the linear amplitude sweep tests. As stated above, three main failure definitions are used to analyze the results of the LAS test on the basis of the VECD approach, the 35% reduction in $G^*\sin(\delta)$ (VECD (35% $G^*\sin(\delta)$)), the peak shear stress (VECD (PSS)), and the peak stored PSE (S-VECD (PSE)).

Kuchiishi et al. (2019) found that the S-VECD (PSE) failure definition generally yields a higher fatigue life compared to VECD (PSS) for both unmodified and modified binders. This discrepancy can be substantial, sometimes three to four times higher, particularly at certain temperatures. It is interesting to note that for unmodified 30/45 binder, the fatigue life exhibits an increase with temperature when using the peak shear stress as the failure definition. However, when using the peak of stored PSE as the failure definition, the fatigue life shows a decrease with temperature, indicating an opposite trend (Fig. 22(a)). Remarkably, this contradiction is not observed in highly polymer-modified binders (HPMB) (Fig. 22(b)). In like manner, Wang et al. (2020) demonstrated a poor correlation between the VECD (35% $G^*\sin(\delta)$) and the S-VECD (PSE) & G^R approach. However, a linear relationship has been found between the VECD (PSS) failure definition and the S-VECD (PSE) & G^R approach. They also noted that the 35% reduction of $G^*\sin(\delta)$ failure definition tends to underestimate fatigue life. Therefore, they recommended using the peak shear stress failure definition in the LAS test.

To highlight the effect of failure definition on the fatigue life prediction, Zhang et al. (2020) investigated the fatigue life of different types of binders, including unmodified and modified binders, as well as unaged and aged binders, using the LAS test with the three mentioned failure definitions. They concluded that the peak shear stress yielded the most accurate predictions. Interestingly, they noted that the peak of stored PSE was not as clearly observed for the modified binders. Conversely, Roque et al. (2020) found that the fatigue lives of unmodified and modified binders were comparable when using the 35% reduction in $G^*\sin(\delta)$ as the failure definition in the LAS test. However, they observed a plateau instead of a distinct peak in the shear stress-strain curves of some polymer-modified binders when using the peak shear stress as the failure definition. Nevertheless, they found that the S-VECD & G^R approach effectively differentiated between unmodified and polymer-modified binders, thus considering the 35% reduction in $G^*\sin(\delta)$ and peak shear stress failure definitions inadequate. Similarly, Yan et al. (2021) showed that, for high-performance modified binders, utilizing S-VECD (PSE) as the fatigue failure definition is recommended. They argued that the current failure definitions used in the LAS test, namely the 35% reduction in $G^*\sin(\delta)$ and peak shear stress, cannot adequately capture the improved performance expected from polymer modifiers.

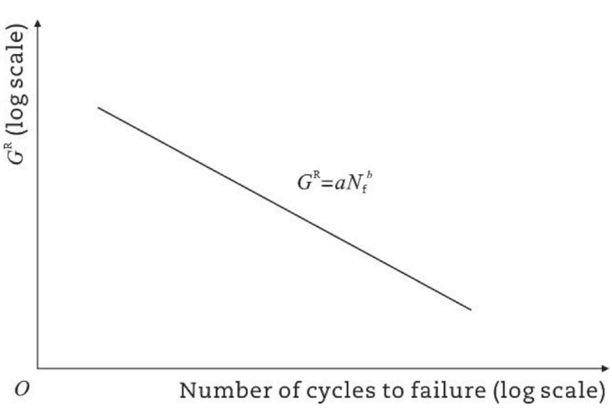

Fig. 21 – Relationship between G^R and N_f (Yan et al., 2021).

Table 1 – Main difference in the VECD approach, based on the pseudo strain energy, the dissipation energy and the G^R approach.

Approach	C	D_f	A	Reference
Peak shear stress	$\frac{\sigma_P}{\epsilon_p^R\,\mathrm{DMR}}$	$\left(\frac{C_0 - C_{\text{at peak stress}}}{C_1}\right)^{\frac{1}{C_2}}$	$\frac{f(D_f)^k}{k(\pi\, C_1 C_2)^{\alpha}}$	Kim et al. (2006)
35% reduction $\lvert G^*\rvert \sin(\delta)$	$\lvert G^*\rvert \sin(\delta)$	$0.35\left(\frac{C_0}{C_1}\right)^{\frac{1}{C_2}}$	$\frac{f(D_f)^k}{k(\pi\, I_D\, C_1 C_2)^{\alpha}}$	Johnson (2010)
50% reduction $\frac{\lvert G_i^*\rvert \sin(\delta_i)}{\lvert G_0^*\rvert \sin(\delta_0)}$	$\frac{\lvert G_i^*\rvert \sin(\delta_i)}{\lvert G_0^*\rvert \sin(\delta_0)}$	$0.5\left(\frac{C_0}{C_1}\right)^{\frac{1}{C_2}}$	$\frac{f(D_f)^k}{k(\pi\, I_D\, C_1 C_2)^{\alpha}}$	Li et al. (2022); Zhang et al. (2020, 2022)
G^R approach	$\frac{\sigma_P}{\epsilon_p^R\,\mathrm{DMR}}$	Maximum stored PSE	$N_f = \left[\frac{K}{a}\,\gamma^{2+2\alpha\left(\frac{C_2}{p}\right)}\right]^{\frac{1}{b+1-\frac{C_2}{p}}}$	Wang et al. (2015)

The authors of this paper utilized the findings reported by Roque et al. (2020) to establish correlations between the three failure definitions. It is evident from the results that there is no significant correlation between the VECD (35% G*sin(δ)) and VECD (PSS) failure definitions (Fig. 23(a) and (b)), nor between the VECD (35% G*sin(δ)) and S-VECD & G^R approach (Fig. 23(c) and (d)) for the predicted fatigue life at 2.5% and 5.0% shear strain. However, a notable correlation was observed between the peak shear stress failure definition and the G^R approach, particularly at 5% shear strain (Fig. 23(e) and (f)).

To compare the effect of failure criterion on the damage characteristic curves, Zhang et al. (2020) used two analytical methods to constitute the damage characteristic curves, the pseudo-strain energy-based method, developed by Wang et al. (2015), and the dissipated energy-based method adopted by Johnson (2010), Johnson and Bahia (2010). They observed differences in the cumulative value of damage intensity (D) and the damage characteristic curves between the two methods (Fig. 24). This discrepancy primarily stems from the theoretical differences in the equations for calculating damage intensity in the two methods. In the pseudo-strain energy-based method, the material integrity C is defined as $C = \frac{\sigma_P}{\epsilon_p^R\,\mathrm{DMR}}$ (Eq. (17)), whereas it is defined as $C = G^*\sin(\delta)$ (Eq. (30)) in the dissipated energy-based method. Additionally, the coefficient $\frac{\mathrm{DMR}}{2}(\epsilon_p^R)^2$ in the damage intensity (Eq. (22)) in the pseudo-strain energy-based method is replaced by the coefficient $\pi I_D \gamma^2$ (Eq. (28)) in the dissipated energy-based method. As the material integrity C is practically identical at the same strain for the two analytical methods (Fig. 24), consequently the main difference in the cumulative value of damage intensity (D) and the damage characteristic curves is attributed essentially to the disparity in the two coefficients $\frac{\mathrm{DMR}}{2}(\epsilon_p^R)^2$ and $\pi I_D \gamma^2$. Therefore, Zhang et al. (2020) recommended the pseudo-strain energy method for representing damage growth.

Based on the findings and conclusions drawn from various reviewed papers, it can be concluded that the simplified viscoelastic continuum damage, based on the peak of stored pseudo strain energy fatigue failure definition proposed by Wang et al. (2015), is the most recommended whatever the bitumen nature, modified and unmodified and aged and unaged binders, and the loading mode and history.

In the TS test, various fatigue failure criteria and failure definitions are utilized to predict the fatigue life of asphalt binders. These include: 50% reduction in complex modulus G*($N_{f50\%}$), the peak in phase angle (PPA), the peak in stiffness ratio (NSR), the dissipated energy ratio (DER), the 20% deviation from the DER undamaged line (N_{p20}), and the ratio of dissipated energy change (RDEC). Wang et al. (2016) compared five fatigue failure definitions using the time sweep fatigue test conducted under control-stress and control-strain mode, the $N_{f50\%}$, the PPA, the peak of NSR, the DER and the RDEC. They found that the RDEC approach, PPA and peak in NSR provide comparable fatigue life predictions, and they recommended the NSR failure criterion because it is well defined and easy to calculate. However, Cao and Wang (2018) discovered that, when using the NSR failure definition, the fatigue life of some aged binders was higher than that of unaged binders, contrary to the experimental evidence and general engineering experience. Consequently, they proposed a new failure definition, defined as the peak of $iC^2(1-C)$, where C is the material integrity aforementioned in Eq. (14). Similarly, Yan et al. (2022) studied the fatigue behavior of multiple modified asphalts binders using four different failure definitions: the $N_{f50\%}$, the PPA, the peak of NSR, and the N_{p20} parameter. They observed that the phase angle and NSR peaks were not applicable to high-performance elastomeric-modified binders. Specifically, no peaks were observed for elastomeric-modified asphalts for both strain levels tested (5% and 10%). The authors found a strong correlation between the 50% reduction in complex modulus and the N_{p20} parameter ($R^2 = 0.96$). Based on their findings, they recommended the 50% reduction in the stiffness modulus as the most suitable failure point.

The TS test was also employed by Bessa et al. (2019) to investigate the fatigue behavior of three asphalt binders: neat penetration grade 30/45 bitumen, modified bitumen with 3% SBS, and highly modified bitumen with 7.5% SBS. They utilized three failure definitions: the reduction in the initial G^* to 50%, NSR, and DER. Interestingly, the authors found that all three failure definitions yielded similar fatigue life results based on their published findings. Similarly, Mannan and Tarefder (2018) demonstrated that there was no significant difference between the 50% reduction in stiffness, DER, and RDEC failure criteria. Furthermore, Nan et al. (2022)

Table 2 – Failure definitions used in the TS and LAS tests.

Author	50% G^*	PPA	SR/NSR	DER/N_{p20}	RDEC	VECD (PSS)	VECD ($G^*\sin(\delta)$)	S-VECD (PSE)
Anderson et al. (2001)				×				
Bonnetti et al. (2002)				×				
Planche et al. (2004)				×				
Shen et al. (2006)					×			
Martono et al. (2007)				×				
Santagata et al. (2009)	×			×	×			
Tabatabaee and Tabatabaee (2010)	×			×				
Johnson (2010)				×			×	
Shen et al. (2010)					×			
Hintz et al. (2011)							×	
Liu et al. (2011)				×				
Wang et al. (2015)								×
Kavussi and Barghabany (2016)						×		
Mannan et al. (2015)							×	
Safaei and Castorena (2016)								×
Wang et al. (2016)	×	×	×	×	×			
Underwood (2016)								×
Saboo and Kumar (2016)						×		
Safaei et al. (2016)								×
Mirhosseini et al. (2017)						×		
Ameri et al. (2017)	×						×	
Xie et al. (2017)								×
Safaei and Castorena (2017)								×
Wang et al. (2018b)								×
Wang et al. (2018a)								×
Cao and Wang (2018)								×
Sabouri et al. (2018)							×	
Safaei and Castorena (2020)								×
Baglieri et al. (2018)								×
Mannan and Tarefder (2018)	×			×	×			
Sun et al. (2019)						×		
Kuchiishi et al. (2019)						×		×
Bessa et al. (2019)	×		×	×		×		
Cao and Wang (2019)								×
Liu et al. (2019)			×		×			
Garcia et al. (2020)				×			×	
Qiu et al. (2020)					×			
Zhang et al. (2020)		×					×	×
Błażejowski et al. (2020)						×		
Roque et al. (2020)						×		×
Morshed et al. (2020)						×		
Wang et al. (2020)								×
Zhang et al. (2022)							×	
Chen et al. (2021)								×
de Oliveira et al. (2021)		×						
Salehfard et al. (2021)								×
Yue et al. (2021)								×
Deef-Allah and Abdelrahman (2021)						×		
Aurilio et al. (2021)							×	
Yan et al. (2021)						×	×	×
Asadi et al. (2021)							×	
Chen et al. (2021)						×	×	×
Kamboozia et al. (2021)						×		
Wang et al. (2021)								×
Zhang and Oeser (2021a)			×	×	×			
Luo et al. (2022)	×			×	×			
Yan et al. (2022)	×	×	×	×				
Yang et al. (2022)								×
Lyu et al. (2022)	×							

(continued on next page)

Table 2 – (*continued*)

Author	50% G^*	PPA	SR/NSR	DER/N_{p20}	RDEC	VECD (PSS)	VECD ($G^*\sin(\delta)$)	S-VECD (PSE)
Nan et al. (2022)	×	×		×		×		
Li et al. (2022)	×			×	×		×	
Wang et al. (2022)	×							×
Chen and Bahia (2022)							×	
Liu et al. (2022)						×		
Steineder et al. (2022)	×	×		×	×	×		
Joohari and Giustozzi (2022)							×	
Wang et al. (2023)								×
An et al. (2023)								×
Total of used failure definitions	13	6	5	18	11	16	15	26

established correlations between the 50% reduction in stiffness (termed as 0.5S), NSR and DER failure definitions. A strong correlation has been founded between DER and NSR, in which the coefficient of correlation R^2 is close to 1 (Fig. 25(a)). Additionally, the 50% reduction in G^* failure definition exhibited a good correlation with both NSR (Fig. 25(b)) and DER (Fig. 25(c)), with an R^2 greater than 0.75.

On the other hand, Luo et al. (2022) found that the RDEC failure criterion and the 50% reduction in G^* are more consistent than the DER approach. They also show that the N_p and N_{p20} parameters determined from the DER approach provide practically the same fatigue life. Indeed, it has been found that the fatigue lives predicted from the RDEC and 50% reduction in G^* are higher than those predicted from the DER approach. Additionally, the loading mode can also affect the correlations between the different failure points. Steineder et al. (2022) demonstrated a strong correlation between the four-failure definitions, 50% reduction in the G^*, peak phase angle, DER and RDEC using the time sweep test under the stress-controlled mode, with a coefficient of determination close to 1. However, in the case of strain-controlled mode, the authors found that the peak phase angle does not correlate well with the author failure points (R^2 < 0.5). The three-failure criterion, 50% reduction in G^*, DER and RDEC, showed good correlation regardless of the loading mode. The authors recommended the utilization of 50% reduction in G^* and DER failure definitions. It was observed that the fatigue life predicted based on the DER approach is about 7%–10% smaller than that predicted with the 50% reduction in G^* (Steineder et al., 2022).

The impact of the applied stress amplitude on the correlation between failure criteria and failure definitions has also been studied. Zhang and Oeser (2021a) showed that, at small applied amplitude, the difference between the fatigue life of asphalt binders predicted based on the DER failure criterion is much higher than that predicted based on the NSR failure criterion. However, this difference decreased when higher amplitudes were tested on the TS test using stress-controlled mode. Additionally, the authors also noted that at high applied amplitudes (as an indication, beyond 700 kPa for 20/30 penetration grade and beyond 250 kPa for SBS modified bitumen), the DER deviates from the undamaged line after only a few load cycles. Consequently, they questioned the utilization of the DER failure criterion at high applied amplitudes.

A multi-criteria analysis was conducted from the reviewed papers regarding the correlation between fatigue failure definitions in the TS test. This analysis, presented in Table 3, assigns a positive sign (+) to the recommended failure definitions or those present a good correlation and a negative sign (−) to criticized failure definitions or those present a poor correlation, regardless of the bitumen's nature or the loading mode used in the TS test. The findings reveal that the traditional 50% reduction in stiffness modulus emerges as the most recommended failure point for predicting asphalt binder fatigue life using the time sweep test, followed by the RDEC approach than the DER failure criterion. Meanwhile, the peak phase angle is deemed less recommended among the compared failure definitions.

6. Correlation between the TS test and LAS test

The LAS test is an accelerated fatigue test, which is considered a surrogate for the TS test (real fatigue test) (Hintz, 2012; Johnson, 2010; Johnson and Bahia, 2010). Several studies compared the fatigue life of asphalt binders using both LAS and TS tests (Cao and Wang, 2019; Nan et al., 2022; Safaei et al., 2016; Yan et al., 2022). A strong correlation between the LAS test and the TS test has been observed by Cao and Wang (2019) when using pseudo-strain energy as a failure definition for both tests (Fig. 26). Furthermore, studies by Wang et al. (2020) and Yan et al. (2022) demonstrated a strong correlation between the TS test, utilizing various failure definitions, and the LAS test based on the S-VECD (PSE). Similarly, Nan et al. (2022) reported a strong correlation (R^2 = 0.83) between the LAS test utilizing peak shear stress as a failure definition and the TS test using the DER approach (Fig. 27). Additionally, Safaei et al. (2016) utilized the S-VECD (PSE) approach to analyze the damage characteristic curves (DCC) for both TS and LAS tests. They showed that the DDC derived from the time sweep test exhibit greater linearity and higher values of material integrity for the same damage intensity compared to those

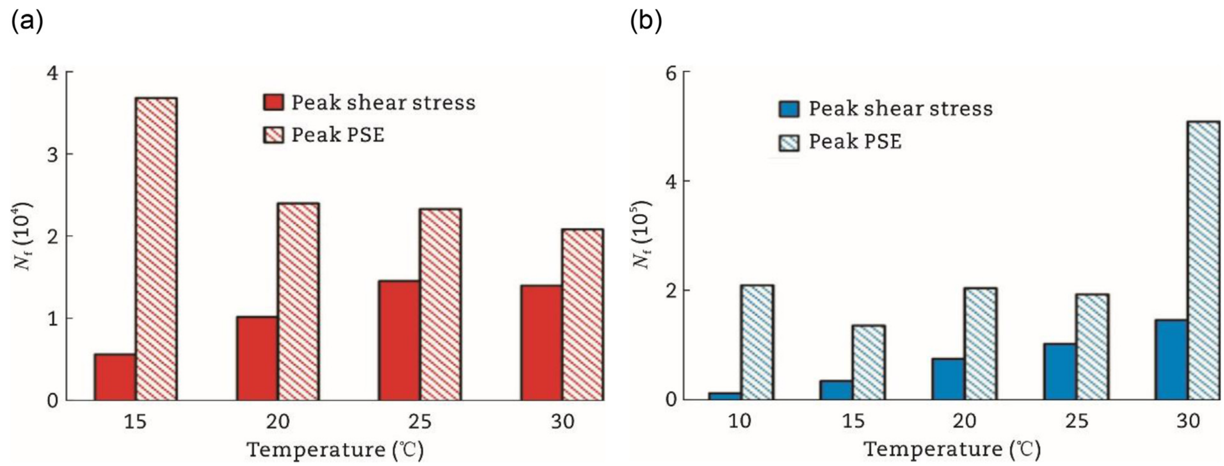

Fig. 22 – Fatigue life based peak shear stress and peak PSE (Kuchiishi et al., 2019). (a) Unmodified binder. (b) HPMB.

generated from the LAS test (Fig. 28). This difference is primarily attributed to material non-linearity induced by the high amplitude of the LAS test, reaching up to 30%.

In summary, the LAS fatigue test demonstrates a strong correlation with the real binder fatigue test (TS test), particularly when employing the S-VECD (PSE) failure definition, regardless of the fatigue test temperature. However, it is essential to note that the fatigue life of asphalt binder is significantly influenced by the fatigue test temperature in both LAS and TS tests, regardless of the failure definition employed.

7. Effect of experimental tests conditions on the fatigue life of asphalt binder

The fatigue test conditions, including test temperature, loading mode, loading time, and gap size, can significantly influence the fatigue life of asphalt binders. Therefore, it is crucial to carefully consider and control these test conditions to obtain accurate and reliable fatigue test results for asphalt binders.

7.1. Effect of fatigue test temperature on the fatigue life of asphalt binder

It is generally assumed that an increase of testing temperature enhances the fatigue life of binders. However, conducting fatigue tests at higher temperatures may lead to an overestimation of the binder's fatigue performance, while testing at lower temperatures may result in underestimation (Kuchiishi et al., 2019). Therefore, the temperature at which fatigue tests are conducted plays a crucial role in evaluating the fatigue life of asphalt binders, and careful selection of the test temperature is essential. Furthermore, Chen et al. (2022) demonstrated that the effect of temperature on the fatigue life of asphalt binder, assessed using the LAS test, is more pronounced at high strain levels compared to low strain levels. As a result, the authors suggested including high strain levels, up to 15%, in the LAS test, rather than the 10% recommended by the AASHTO TP101.

As stated in the literature (Kuchiishi et al., 2019; Safaei and Castorena, 2016; Yang et al., 2023), there are three primary failure mechanisms, cohesive fatigue "true fatigue", adhesion loss (between the rheometer plate and the samples) and instability plastic flow (edge fracture). The edge fracture is the inability of the binder to maintain its geometry at its boundary. Studies by Anderson et al. (2001) and Planche et al. (2004) have demonstrated that, under the same controlled strain in the TS test, the fatigue life of binders increases with temperature and decreases after reaching a maximum value. The temperature at which the fatigue life reaches the peak value is defined as the transition between the fatigue cracking (internal micro-damage) and the instability flow (Fig. 29). These studies indicate that fatigue cracking, also known as true fatigue, tends to occur at temperatures where the initial stiffness modulus exceeds 15 MPa. On the other hand, edge becomes dominant at temperatures where the initial complex modulus is around 5 MPa (Anderson et al., 2001; Planche et al., 2004).

Based on their experimental study with four bitumens, including modified and unmodified bitumens, Safaei and Castorena (2016) established limits for each failure mechanism, adhesion loss for $G^* > 60$ MPa, cohesive fatigue for 12 MPa $\leq G^* \leq$ 60 MPa and plastic flow for $G^* < 12$ MPa, where G^* is measured at LVE domain (low controlled-strain or stress). According to their findings, temperatures corresponding to a complex modulus greater than 60 MPa or less than 12 MPa should be excluded from fatigue testing. Despite this recommendation, several researchers characterized the fatigue life of different binder types at a single intermediate temperature, typically ranging between 20 °C and 25 °C (Asadi et al., 2021; Baglieri et al., 2018; Bessa et al., 2019; Chen et al., 2021; Joohari and Giustozzi, 2022; Liu et al., 2019; Mannan and Tarefder, 2018; Qiu et al., 2020; Sabouri et al., 2018; Salehfard et al., 2021; Shen and Sutharsan, 2011; Sun et al., 2019; Wang et al., 2018b; Yan et al., 2021; Zhang et al., 2020; Zhang and Oeser, 2021a).

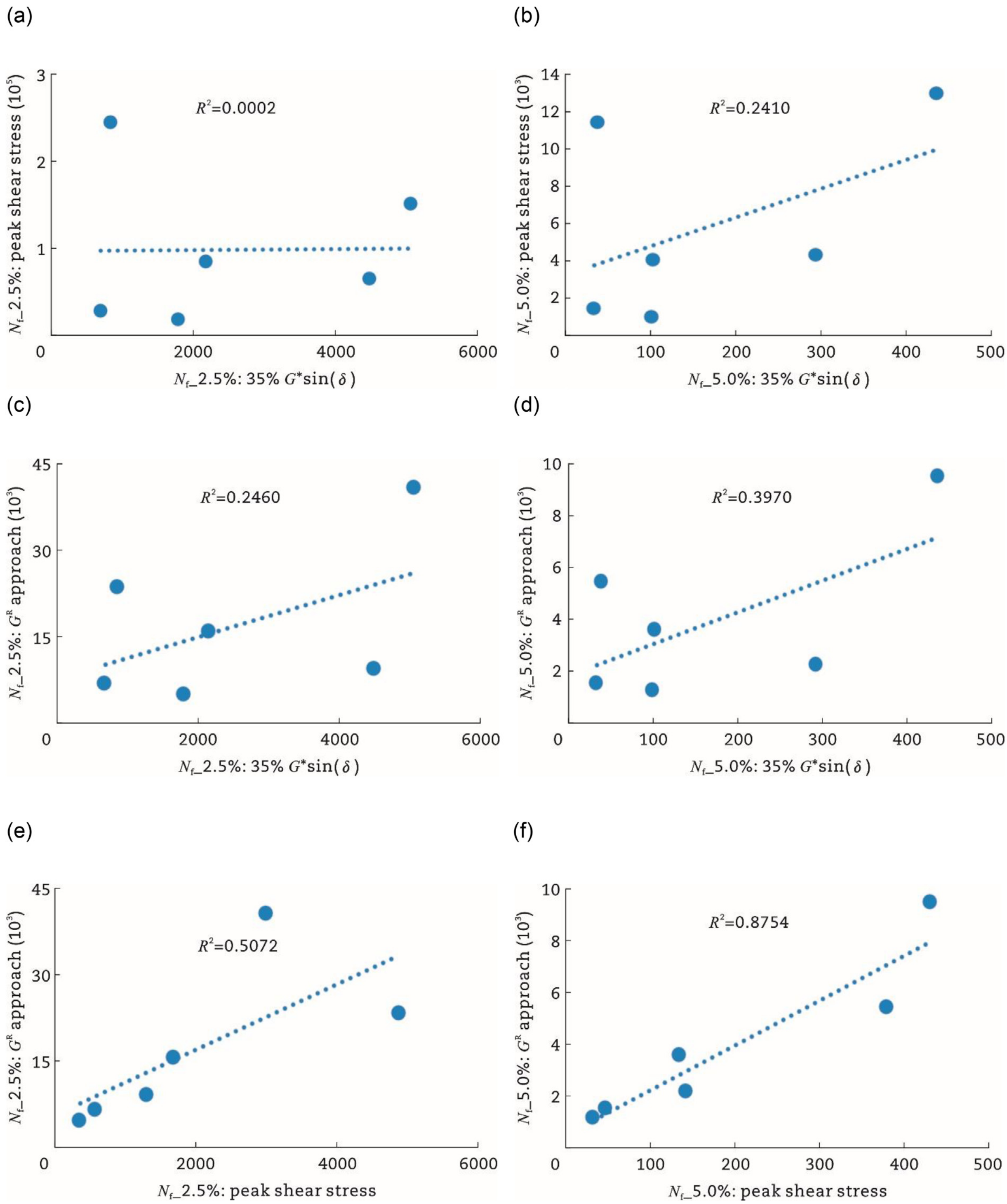

Fig. 23 – Correlations between failure definitions (Roque et al., 2020). (a) N_f at 2.5%_35% $G^*\sin(\delta)$ Vs. PSS. (b) N_f at 5.0%_35% $G^*\sin(\delta)$ Vs. PSS. (c) N_f at 2.5%_35% $G^*\sin(\delta)$ Vs. G^R. (d) N_f at 5.0%_35% $G^*\sin(\delta)$ Vs. G^R. (e) N_f at 2.5%_PSS Vs. G^R. (f) N_f at 5.0%_PSS Vs. G^R.

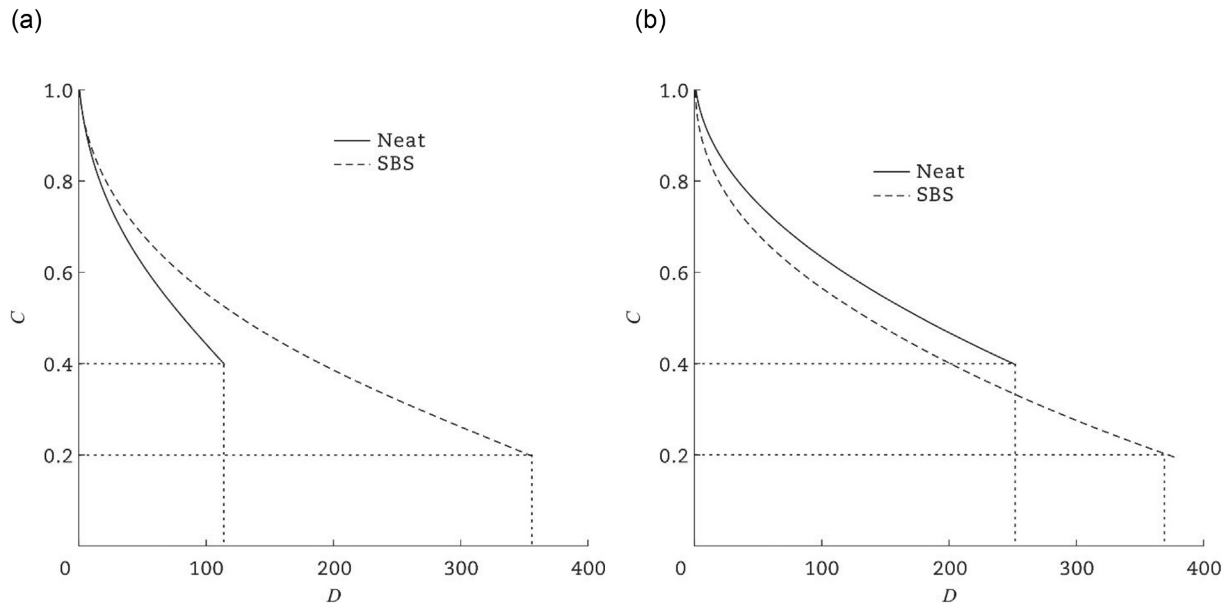

Fig. 24 – Damage characteristic curves (Zhang et al., 2020). (a) Dissipated energy. (b) Pseudo-strain energy-based method.

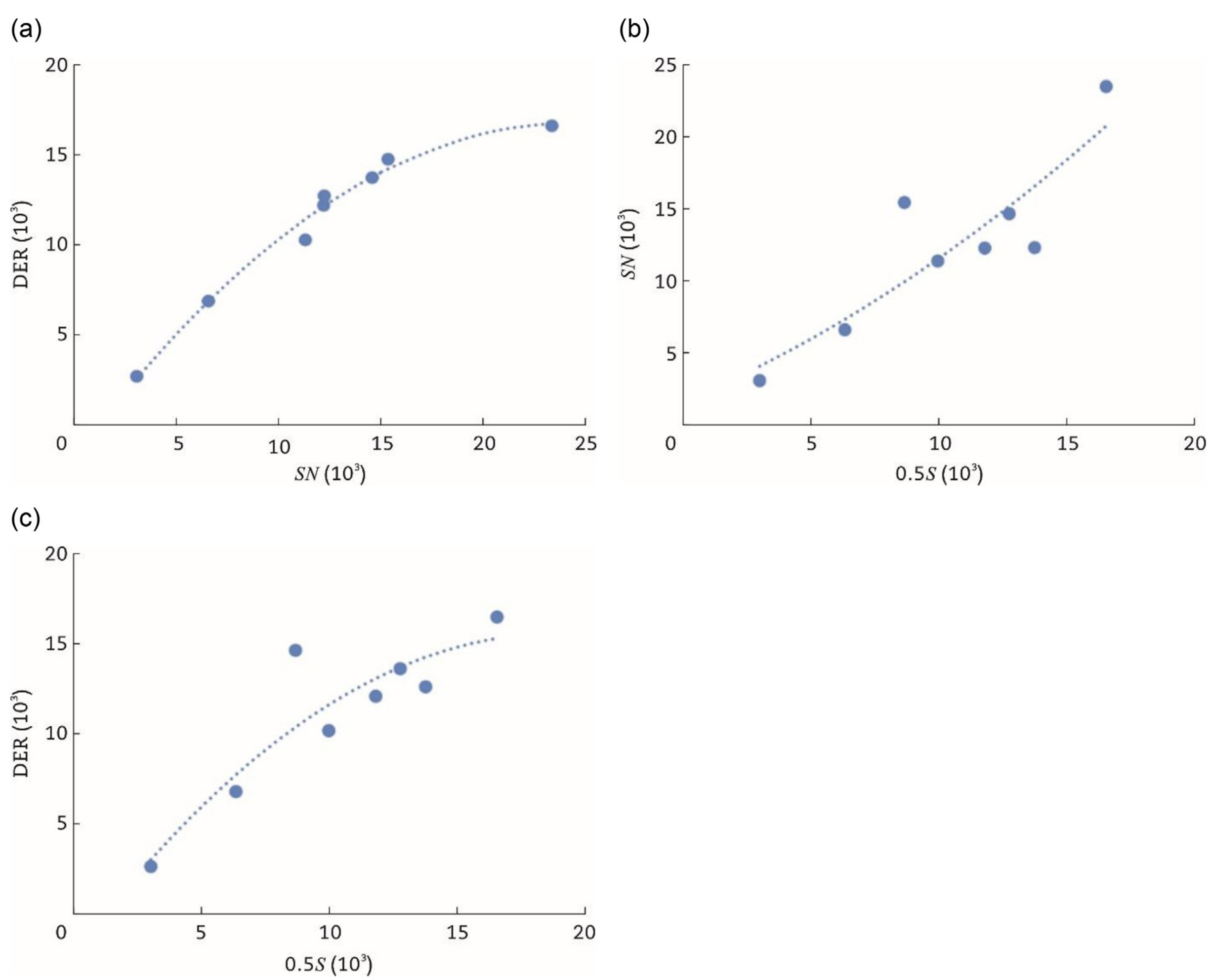

Fig. 25 – Correlation between 0.5S, DER and NSR failure criteria in the time sweep test (Nan et al., 2022). (a) SN Vs. DER. (b) 0.5S Vs. SN. (c) 0.5S Vs. DER.

Table 3 – Multi-criteria analysis to define the most recommended failure definitions.

Reference	50% G^*	PPA	NSR	DER/N_{p20}	RDEC
Wang et al. (2016)		+	+		+
Cao and Wang (2018)			−		
Mannan and Tarefder (2018)	+			+	+
Bessa et al. (2019)	+		+	+	
Zhang and Oeser (2021a)			+	−	
Nan et al. (2022)	+		+	+	
Luo et al. (2022)	+			−	+
Yan et al. (2022)	+	−	−	+	
Steineder et al. (2022)	+	−		+	+
Score	+6	−1	+2	+3	+4

Kuchiishi et al. (2019) investigated the impact of temperature variations (ranging from 10 to 30 °C) on the fatigue life of asphalt binders assessed through the LAS test. Two asphalt binders were tested: unmodified 30/45 penetration grade and highly polymer-modified binder. Their findings revealed that both tested binders exhibited cohesive fatigue failure at temperatures of 15 °C and 20 °C. However, plastic flow failure was observed at 30 °C for the unmodified bitumen and at 25 °C for the highly polymer-modified bitumen. Adhesion loss was only detected for the unmodified bitumen at 10 °C, where the base binder displayed higher stiffness compared to the highly polymer-modified binder. Based on their results, the authors recommended a temperature of 20 °C for conventional binders and 15 °C for highly modified binders to assess fatigue performance effectively. Other researchers have used the intermediate temperature performance grade, calculated as the average of the high and low-performance grade temperatures +4 °C (Aurilio et al., 2021; Bonnetti et al., 2002; Chen et al., 2022; Hintz et al., 2011; Wang et al., 2015, 2016). While, certain studies (Santagata et al., 2009; Shenoy, 2002) have utilized the iso-stiffness (or equi-stiffness) temperature

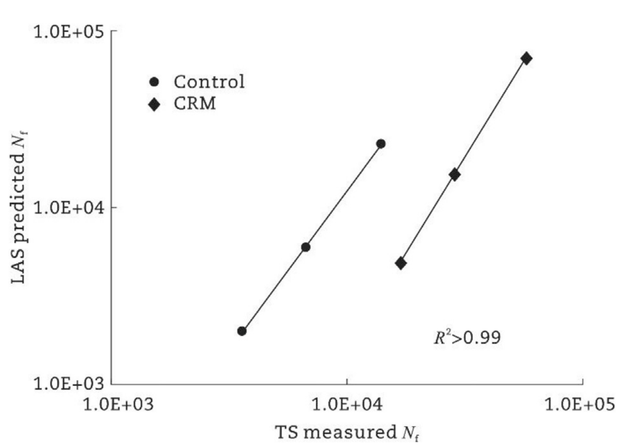

Fig. 26 – Correlation between N_f of TS and LAS tests based on the PSE failure criterion on neat bitumen (control) and bitumen modified with crumb rubber (CRM) (Cao and Wang, 2019).

concept, wherein the test temperature is chosen to ensure that the binders exhibit identical initial complex moduli at the start of the fatigue test, as shown in Fig. 30.

On the basis of this concept, Shenoy (2002) defined the fatigue test temperature at which every tested binder presents a shear complex modulus of 1 MPa at the start of the time sweep fatigue test under a controlled strain of 25%. According to Shenoy (2002), using the 25% controlled strain generate reliable fatigue responses in reasonably short experimental time and consequently avoids the edge fracture even at temperatures correspond to low complex modulus (<1 MPa). In contrast, the conventional time sweep fatigue test, conducted over an extended period, may lead to edge fracture at complex moduli lower than 5 MPa (Martono et al., 2007; Planche et al., 2004). Bonnetti et al. (2002) and Santagata et al. (2009) also adopted the iso-stiffness temperature concept to determine the temperature for fatigue testing, where the initial complex modulus of the binders was set at 15 and 25 MPa, respectively. In another study, Canestrari et al. (2015) utilized an iso-stiffness level of 3 MPa to investigate the fatigue and healing properties of four different binders. They ensured the absence of edge fracture by monitoring the normal force and inspecting the specimens during the fatigue test. Yang et al. (2022) selected the iso-stiffness conditions at 30 MPa, aiming to maintain the complex modulus within the range of 12–60 MPa, as suggested by Safaei and Castorena (2016) to avoid adhesion loss or edge flow.

Johnson (2010) proposed a novel definition of the iso-stiffness temperature concept by incorporating both modulus and phase angle considerations. In this approach, the fatigue test temperature is determined such that $G^*\sin(\delta)$ parameter equals 5 MPa, which corresponds to the fatigue Superpave specification limit. Hintz and Bahia (2013) adopted the same concept proposed by Johnson (2010), but aimed for a target $G^*\sin(\delta)$ value of 6.5 MPa to define the iso-stiffness temperature specifically for conducting the LAS test.

In order to eliminate the effect of fatigue test temperature on the fatigue life on asphalt binders, Safaei and Castorena (2016) applied the time-temperature superposition principle to predict the fatigue performance under any temperature and loading using the LAS test results carried out at one selected temperature. The time-temperature superposition principle has been used, firstly for asphalt concrete (Chehab et al., 2002; Underwood et al., 2006), to eliminate the temperature effect using the S-VECD by the utilization of the reduced time (ξ) rather than the real-time (t) in the damage model (Eq. (41)). The reduced time is calculated using the viscoelastic time-temperature shift factors (Eq. (42)).

$$D(t)=\sum_{i=1}^{n}\left[\frac{\mathrm{DMR}}{2}\left(\gamma_{\mathrm{P}}^{\mathrm{R}}\right)^{2}(C_{i-1}-C_{i})\right]^{\frac{\alpha}{\alpha+1}}(\xi_{i}-\xi_{i-1})^{\frac{1}{1+\alpha}} \tag{41}$$

$$\xi=\frac{t}{a_T} \tag{42}$$

where a_T is the time-temperature shift factor determined from LVE characterization.

In summary, the lack of uniformity in selecting fatigue test temperatures for asphalt binders is evident, highlighting the

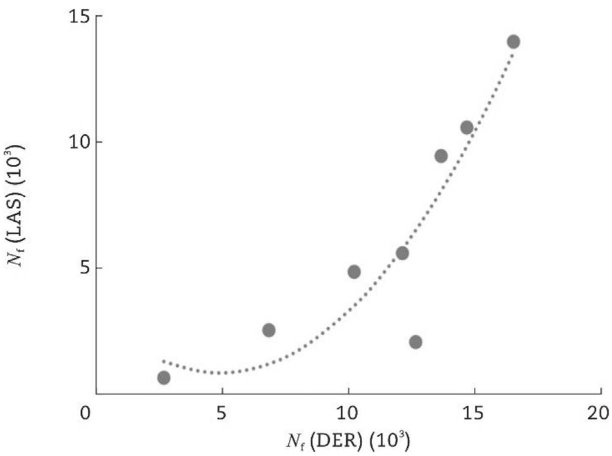

Fig. 27 – Correlation between N_f of LAS test and TS test based on DER criterion (Nan et al., 2022).

need for further investigations to standardize and normalize the selection of fatigue test temperatures for asphalt binders. Table 4 summarizes the various testing temperatures adopted in the literature to investigate the fatigue life of asphalt binders using both TS and LAS tests.

7.2. Effect of fatigue test loading mode on the fatigue life of asphalt binder

Luo et al. (2022) evaluated the fatigue life of asphalt binders using the time sweep test under various stress-controlled modes. It has been demonstrated that the fatigue life decreases when the applied stress increase, whatever the failure criterion used, as shown in Fig. 31.

As for the effect of loading mode, Johnson (2010) conducted the LAS test under controlled stress mode rather than controlled strain mode. At each loading interval, the stress was increased by 50 kPa until 1000 kPa. Under stress-controlled mode, the strain response increases with damage. However, in strain-controlled mode, the stress response decreases with damage (Fig. 32). It has been found that the strain-controlled mode gives a peak shear stress response during the damage with a decrease in material integrity. However, without a priori knowledge, the stress-controlled mode gives abrupt failure. According to Johnson (2010), the predicted fatigue life under the strain-controlled mode is more accurate.

7.3. Effect of fatigue test duration on the fatigue life of asphalt binders

As for the effect of loading time on the fatigue life of asphalt binders, Wang et al. (2015) conducted the LAS test under different duration by changing the constant strain-amplitude rates (CSR). The CSR is defined as the strain amplitude (%) divided by the test duration. For the standard LAS test, with a duration of 5 min (LAS-5), the CSR equals 0.00100 (30%/300). The various CSR tested is 0.00400 (LAS-1.25), 0.00200 (LAS-2.5), 0.00100 (LAS-5), 0.00050 (LAS-10) and 0.00033 (LAS-15) (Fig. 33). Similarly, Wang et al. (2020) and Roque et al. (2020) evaluated the fatigue life of various asphalt binders using the LAS test with different durations (LAS-5, LAS-10 and LAS-15) on the basis of S-VECD and G^R approach. As a result, Wang et al. (2020) showed that the standard LAS test (LAS-5) correlates very well with the time sweep. While, Roque et al. (2020) demonstrated that there is less damage per loading cycle in the case of long loading time (LAS-15), resulting in an increase in fatigue life (Fig. 34).

7.4. Effect of gap size on the fatigue life of asphalt binders

Anderson et al. (2001) investigated the impact of the gap size (1, 2 and 3 mm) on the fatigue life of asphalt binders using

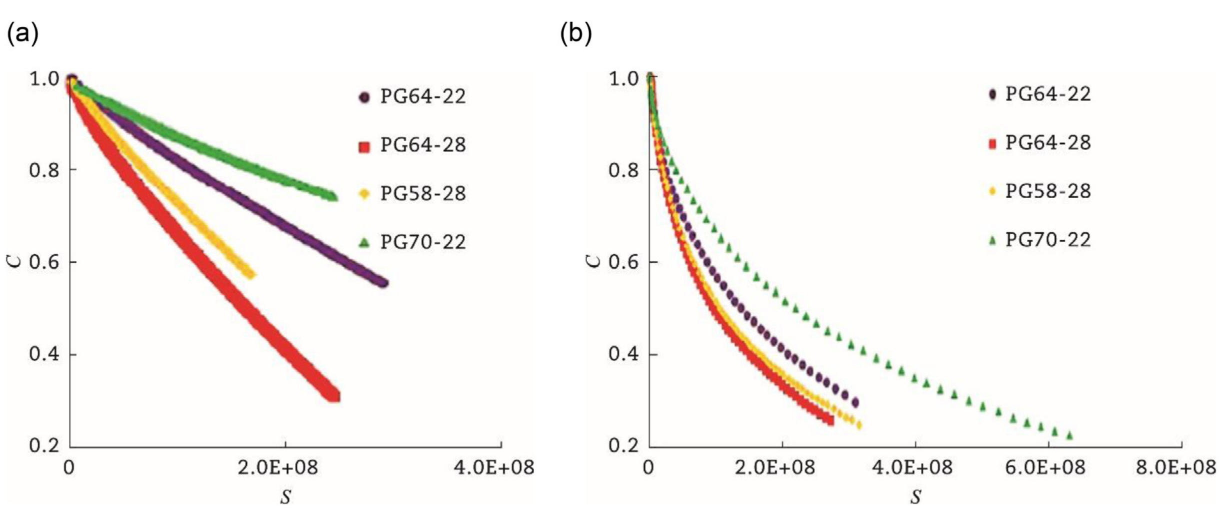

Fig. 28 – Damage characteristic curves (Safaei et al., 2016). (a) TS test. (b) LAST test.

Table 4 – The fatigue test temperatures adopted in the literature using LAS and TS tests.

Testing temperature		Test (LAS/TS)	Reference
Arbitrary intermediate temperatures	20 °C	LAS/TS	Baglieri et al. (2018); Bessa et al. (2019); Mannan and Tarefder (2018); Sun et al. (2019); Wang et al. (2018b); Yan et al. (2021)
	25 °C	LAS/TS	Asadi et al. (2021); Chen et al. (2022); Joohari and Giustozzi (2022); Liu et al. (2019); Qiu et al. (2020); Sabouri et al. (2018); Salehfard et al. (2021); Shen and Sutharsan (2011); Zhang et al. (2020); Zhang and Oeser (2021a)
	10 °C, 15 °C, 20 °C and 30 °C	LAS	Kuchiishi et al. (2019)
Intermediate temperature performance grade		LAS/TS	Aurilio et al. (2021); Bonnetti et al. (2002); Chen et al. (2022); Hintz et al. (2011); Wang et al. (2015, 2016)
Iso-stiffness temperature	$G^* = 1$ MPa	TS (strain = 25%)	Shenoy (2002)
	$G^* = 3$ MPa	TS (strain = 5%)	Canestrari et al. (2015)
	$G^* = 15$ MPa	TS (strain = NM*)	Bonnetti et al. (2002)
	$G^* = 25$ MPa	AS*	Santagata et al. (2009)
	$G^* = 30$ MPa	LAS/TS (strain = 2%–6%)	Yang et al. (2022)
	$G^*\sin(\delta) = 5$ MPa	LAS	Johnson (2010)
	$G^*\sin(\delta) = 6$ MPa	LAS	Hintz and Bahia (2013)
Cohesive fatigue temperature	$12 \text{ MPa} \le G^* \le 60$ MPa	LAS	Safaei and Castorena (2016)
Time-temperature superposition principle		LAS	Safaei and Castorena (2016)

Note: NM means not mentioned, AS means amplitude sweep until 100% strain.

the TS test. Their findings revealed that for cohesive fatigue, where failure is attributed only to internal damage, the fatigue life remains unaffected by the gap size. However, in the case of instability plastic flow, the fatigue life is significantly influenced by the thickness of the gap (Fig. 35).

7.5. *Effect of damage evolution rate parameter α on the fatigue life of asphalt binders*

Safaei et al. (2016) conducted a comparative analysis to evaluate the impact of the damage evolution rate parameter, α ($\alpha = 1/m$ and $\alpha = 1 + 1/m$), on the damage characteristic curves (DCCs) of asphalt binders using the time sweep test based on the S-VECD. Their findings revealed distinct behavior in the DCCs based on the chosen α parameter. When $\alpha = 1/m$ was utilized, the DCCs exhibited loading history and temperature dependence (Fig. 36(a)). In contrast, when $\alpha = 1 + 1/m$ was utilized, the DCCs displayed no dependency on temperature and loading history (Fig. 36(b)). Consequently, Safaei et al. (2016) recommended adopting $\alpha = 1 + 1/m$ for characterizing damage evolution in asphalt binders.

Still on the effect of damage evolution rate parameter α on the fatigue life of asphalt binders, Johnson (2010) conducted a comparative analysis between the α calculated from the frequency sweep (first step in the LAS test) and the α calculated from the stress relaxation test. The study revealed a significant correlation ($R^2 > 0.98$) between the fatigue life predictions obtained from the LAS test and those from the time sweep test when α was calculated based on the frequency sweep test results. In contrast, a poor correlation was observed when α was derived from the stress relaxation test (Fig. 37). These findings suggest that the α parameter calculated from the frequency sweep test is more reliable and is therefore recommended for use in the LAS test to predict asphalt binder fatigue life accurately.

Based on the findings presented above, Table 5 summarizes the impact of experimental test conditions on fatigue testing of asphalt binders.

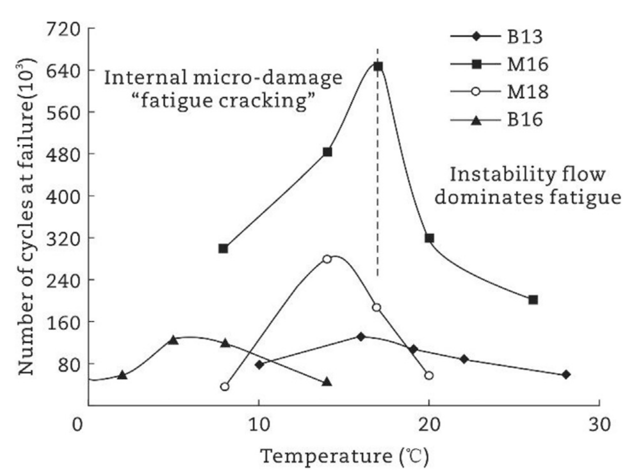

Fig. 29 – Variation of fatigue life with temperature for different binders using the TS test (Planche et al., 2004).

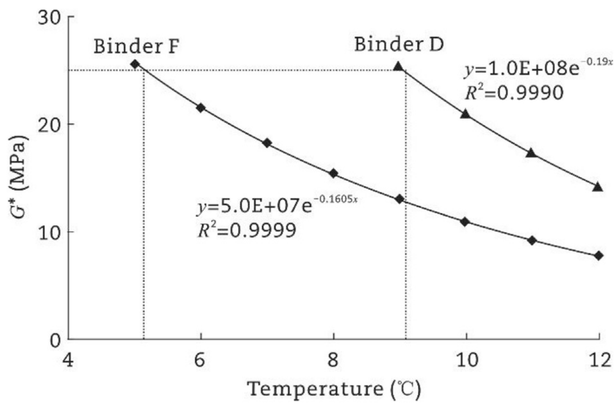

Fig. 30 – Selection of iso-stiffness temperature (Santagata et al., 2009).

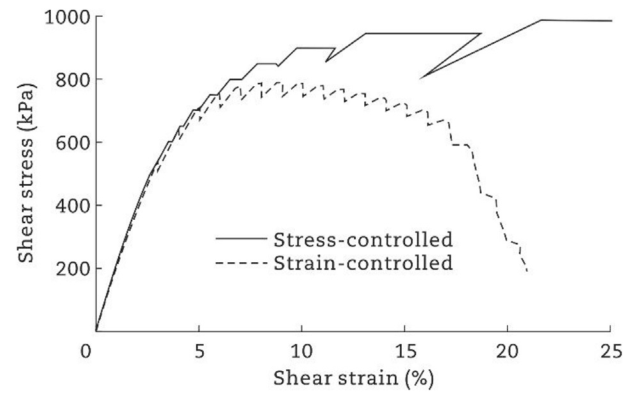

Fig. 32 – Variation of shear stress with shear strain in the LAS test under both stress and strain-controlled mode (Johnson, 2010).

8. Effect of the chemical composition and/or penetration grade of asphalt binder on the fatigue life

Santagata et al. (2009) conducted a comprehensive study on the fatigue and healing properties of six 70/100 penetration grade bitumens sourced from various refineries, each with distinct chemical composition, using the TS test. The researchers investigated the influence of chemical composition, particularly the saturates, aromatics, resins, and asphaltenes (SARA) fractions, on asphalt binder fatigue behavior. Their findings indicated that asphaltenes and saturates could have a beneficial effect on retarding microcrack growth. This positive influence may be attributed to the bodying effect provided by asphaltenes and the flocculation effects resulting from the presence of aliphatic chains within the saturates fraction. However, in contrast to their findings, Wang et al. (2018b) showed that the asphaltene negatively affects the binder fatigue life using the LAS test. They highlighted that the softer binders with higher penetration values exhibit higher fatigue resistance. This observation aligns with the results presented by Cao and Wang (2019), who found that the addition of waste cooking oil, which softens the binder, led to increased fatigue life (Fig. 38). These findings collectively support the notion that softer binders tend to demonstrate higher fatigue lives compared to harder binders.

Salehfard et al. (2021) observed correlations between binder fatigue life and the colloidal instability index (Ic), calculated from SARA fractions, but only when Ic was below 0.9, indicating a threshold limit. Regarding self-healing, Sun et al. (2017) demonstrated that the binders with higher aromatics content exhibited better self-healing ability, while those with higher content of large molecule size showed lower self-healing ability. Similarly, Santagata et al. (2009) and Wang et al. (2018b) highlighted the role of the saturates-to-aromatics ratio in the self-healing of microcracks. Johnson (2010) noted that understanding the relationships between chemical components and mechanical properties of asphalt binders remains challenging.

In order to highlight the effect of penetration grade on the fatigue life of asphalt binders, the authors of this paper utilized

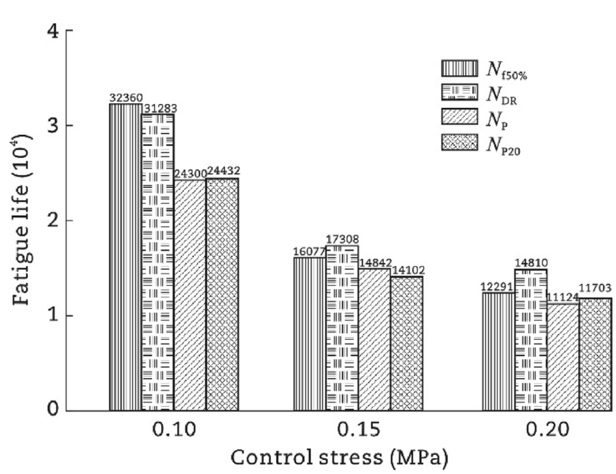

Fig. 31 – Fatigue life under different applied stress (Luo et al., 2022).

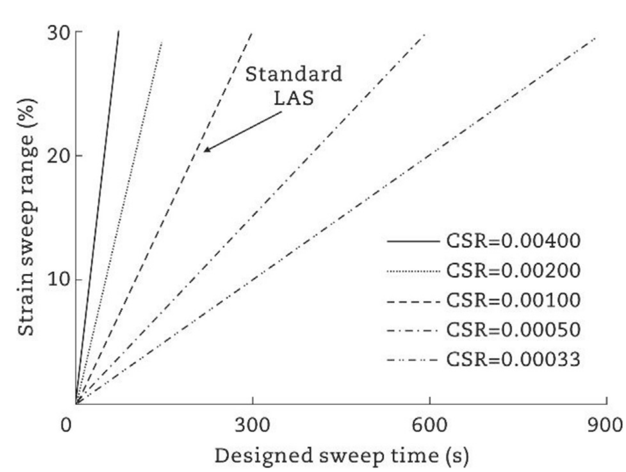

Fig. 33 – LAS test with different loading time (Wang et al., 2015).

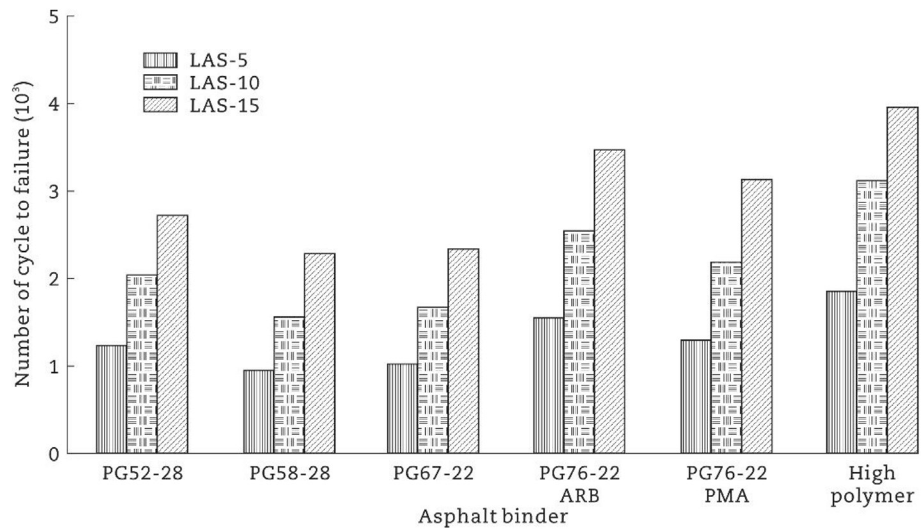

Fig. 34 – Effect of loading time on the fatigue life of asphalt binder using the LAS test (Roque et al., 2020).

data from Liu et al. (2019) research paper, in which the fatigue life of three penetration grades, 50, 70 and 90 were investigated under three level of controlled stress, 70, 80 and 90 kPa using two failure definitions, 50% reduction in G^* and the peak of NSR, as shown in Fig. 39(a) and (b) respectively. A notable observation is that, in particular at lower applied stress levels, the 50-penetration grade bitumen consistently demonstrates significantly higher fatigue life, approximately three times greater, compared to the 70 and 90 penetration grade binders across all failure criteria and controlled stress levels. However, as the applied stress increases, the fatigue life of the 50 penetration grade bitumen decreases considerably compared to the 70 and 90 penetration grade binders, suggesting that at high applied stress levels, the fatigue life of the 70 and 90 penetration grade binders may exceed that of 50 penetration grade bitumen. Liu et al. (2019) did not provide an explicit explanation for the substantial difference in fatigue life among 50, 70 and 90 penetration grade binders. Similarly, Wang et al. (2018b) pointed out that, contrary to expectations, 50 penetration grade bitumen exhibited slightly superior fatigue resistance than 70 penetration grade bitumen due to its lower asphaltenes fraction.

In summary, the development of damage and microcracks within the asphalt binder is also strongly influenced by its

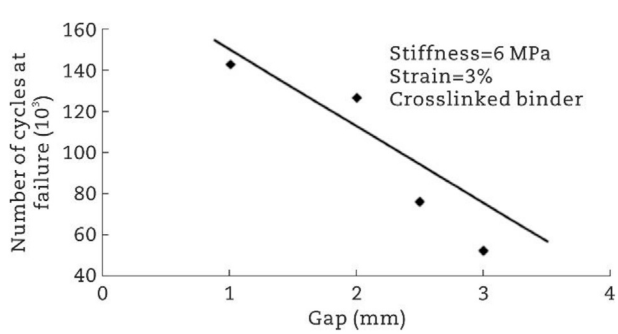

Fig. 35 – Effect of gap size on the fatigue life of asphalt, in the case of instability plastic flow (Anderson et al., 2001).

microstructure. Typically, softer binders demonstrate greater fatigue resistance. However, further research on the impact of bitumen chemistry on fatigue life is needed.

9. Effect of modifiers addition on the fatigue life of asphalt binder

The effect of bitumen modification with various additives on the fatigue life of asphalt binders has indeed been extensively studied, in the literature, using both the TS and LAS tests. Numerous studies have shown the positive effect of various additives on the fatigue behavior of bitumens, the lack of consistency in the testing methods and failure criteria/definitions used makes it challenging to conduct a quantitative and objective comparison across studies. Indeed, several studies (Ameri et al., 2017; Cao and Wang, 2019; Shi et al., 2022; Tabatabaee and Tabatabaee, 2010) have demonstrated the significant improvement in fatigue life with the addition of crumb rubber to bitumen. Similarly, highly-polymer modified binders have shown superior fatigue performance compared to pure bitumen across various temperature conditions (Bessa et al., 2019; Błażejowski et al., 2020; Kuchiishi et al., 2019). This improvement is attributed to the enhanced elasticity provided by the continuous polymeric network in the modified binder, allowing it to resist higher strain levels before failure. Additionally, Saboo and Kumar (2016) and Yan et al. (2022) demonstrated that elastomeric-modified asphalt have higher fatigue life compared to non-elastomeric ones. This improvement is further validated by Aurilio et al. (2021) demonstrating a linear increase in fatigue life with increasing SBS content (Fig. 40). Additionally, observations of failure morphology indicate that damage predominantly occurs in the base binder at the edge of specimens, while the SBS network in the middle remains intact (Zhang and Oeser, 2021b). Furthermore, the combination of crumb rubber (CR) and SBS modification enhances fatigue life compared to the CR-modified bitumen

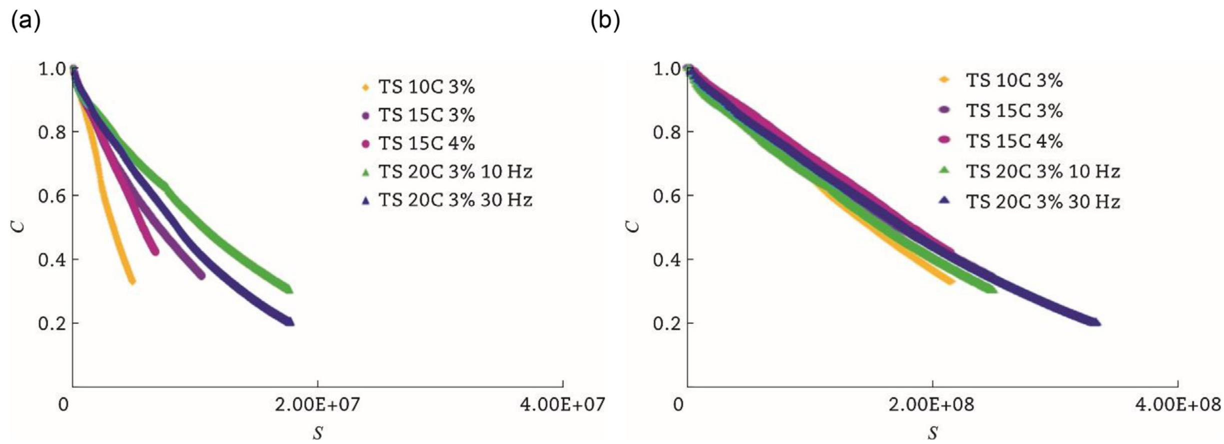

Fig. 36 – Damage characteristic curves of PG 64-28 asphalt binder (Safaei et al., 2016). (a) $\alpha = 1/m$. (b) $\alpha = 1 + 1/m$.

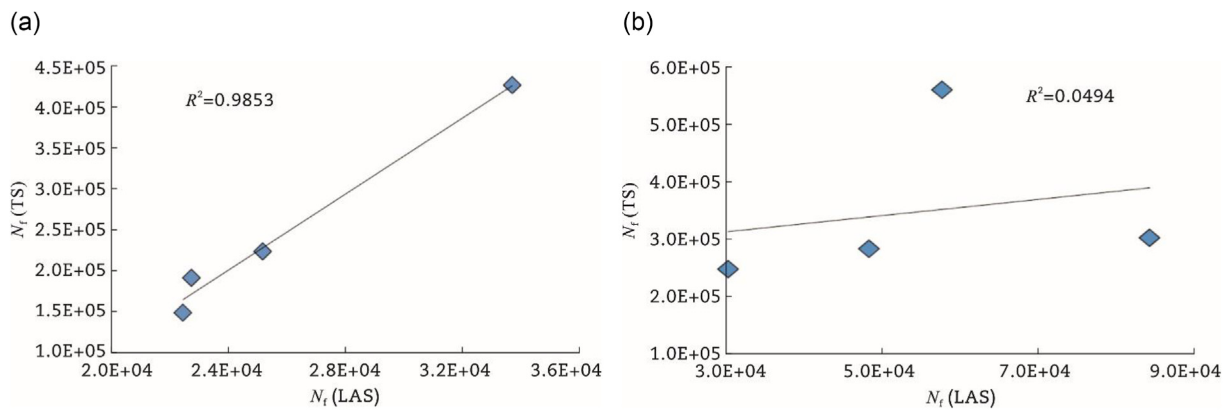

Fig. 37 – Relationship between N_f TS test (3% strain) and the LAS test (Johnson, 2010). (a) α calculated from the frequency sweep. (b) α calculated from the stress relaxation test.

and SBS-modified bitumen, regardless of the failure definitions used, as illustrated in Fig. 41 (Nan et al., 2022).

Yet, the addition of Sasobit® (a synthetic hard wax) in asphalt binders modified with SBS and CR has been investigated by Yue et al. (2021). Their study revealed a substantial improvement in fatigue resistance with the inclusion of Sasobit®. Specifically, the asphalt modified with 3% SBS, 10% CR, and 3% Sasobit® exhibited higher fatigue life across all strain amplitudes.

The effect of adding nanoparticles such as carbon nanotubes and nanoclays (Santagata et al., 2015), organo-montmorillonite (Liu et al., 2011) and nano-hydrated lime

Table 5 – Recommended test conditions for the LAS test.

Testing parameter	Test (LAS/TS)	Observation	Reference
Applied stress	TS	The fatigue life decreases when the applied stress increases.	Luo et al. (2022)
Stress/strain-controlled mode	LAS	The strain-controlled mode is more accurate.	Johnson (2010)
Loading time	LAS	The standard LAS test (LAS-5 min) correlates very well with the time sweep.	Wang et al. (2020)
Gap size	TS	The fatigue life remains unaffected by the gap size in the case of cohesive fatigue.	Anderson et al. (2001)
Damage evolution rate α	LAS	The damage characteristic curves display no dependency on temperature and loading history for $\alpha = 1 + 1/m$.	Safaei et al. (2016)
		The α parameter calculated from the frequency sweep test is more reliable and correlates very well with the time sweep.	Johnson (2010)

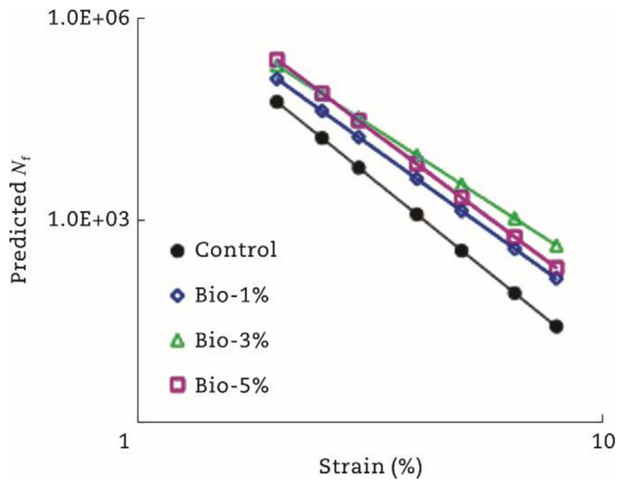

Fig. 38 – Effect of waste cooking oil "termed as Bio" on the fatigue life of asphalt binders (Cao and Wang, 2019).

(Kavussi and Barghabany, 2016), on the fatigue life of asphalt binders was also investigated. Generally, the addition of nanoparticles has been found to improve the fatigue life of asphalt binders, although the efficiency depends on the specific physicochemical properties of the nanoparticles. Also, according to Mirhosseini et al. (2017), the date seed ash significantly improves the fatigue life resistance of asphalt binders. Similarly, An et al. (2023) demonstrated that the addition of graphene oxide enhances the fatigue life of asphalt binders. However, Li et al. (2022) reported that the addition of diatomite had an adverse effect on the fatigue life of asphalt binders, as indicated in Fig. 42. According to the authors, this decrease in fatigue life observed on the diatomite-modified binders is primarily attributed to the increase in the heat dissipation energy caused by the addition of diatomite.

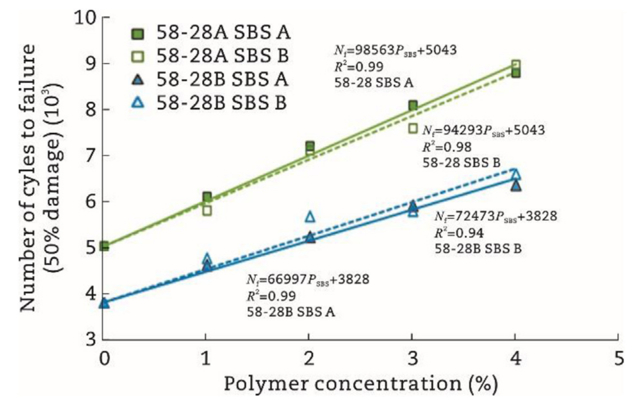

Fig. 40 – Effect of SBS content on the fatigue life of asphalt binders (Aurilio et al., 2021).

Liu et al. (2022) investigated the effect of adding waste engine oil (WEO) and polyphosphoric acid (PPAc) on the fatigue behavior of asphalt binders. Their findings revealed a significant enhancement in fatigue life, with approximately a 1000% increase for 2% PPA + 2% WEO and about a 1150%

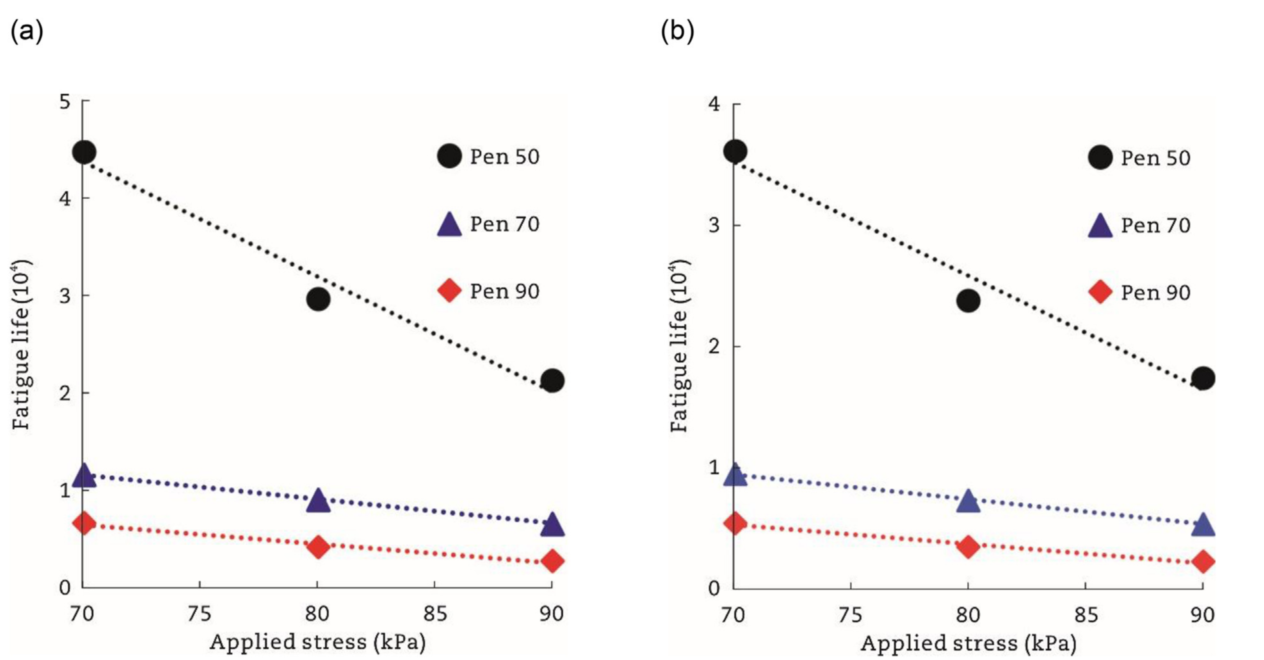

Fig. 39 – Fatigue life of 50, 70 and 90 penetration grade binders (Liu et al., 2019). (a) Failure definition: $N_{f50\%}$ G^*. (b) Failure definition: peak NSR.

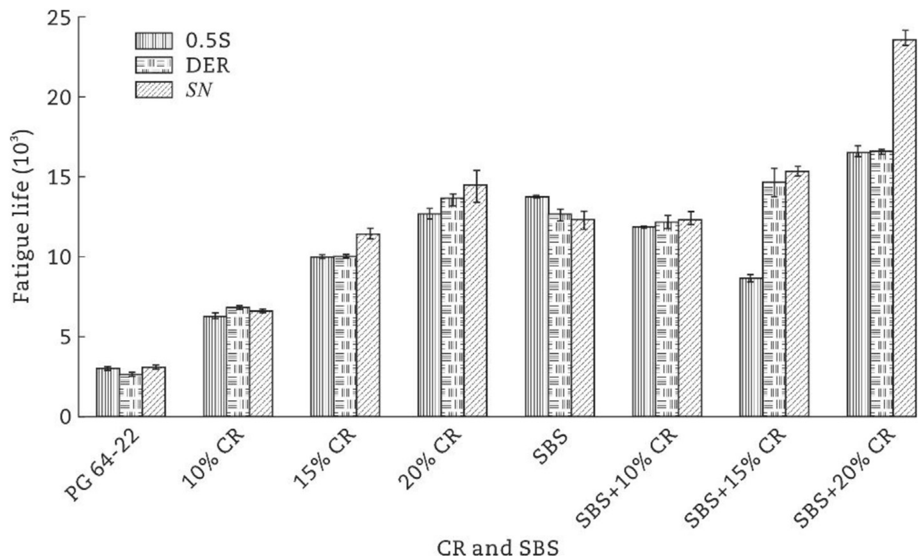

Fig. 41 – Effect of CR and SBS on the fatigue life of modified asphalt binders (Nan et al., 2022).

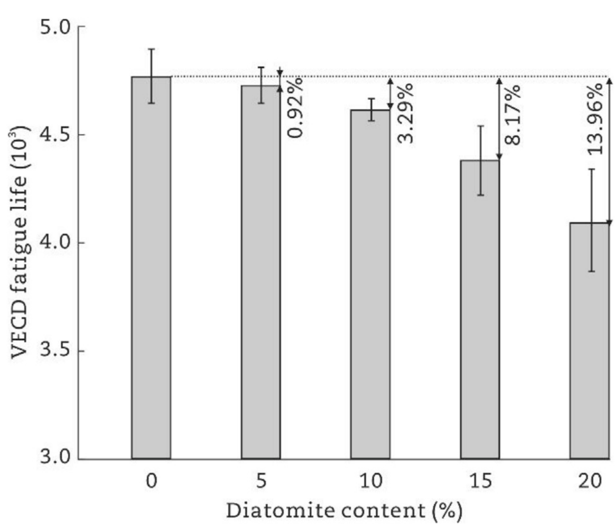

Fig. 42 – Effect of diatomite addition on the fatigue life of asphalt binder (Li et al., 2022).

increase for 1% PPAc + 4% WEO. Similarly, Asadi et al. (2021) found that adding aromatic extract and waste cooking oil rejuvenators improved the fatigue life of aged asphalt binders. The partial replacement of bitumen with a renewable bio-oil resulted in nearly identical fatigue performance compared to virgin bitumen, having the same consistency, as indicated by Gaudenzi et al. (2020). However, they observed that the bio-binder exhibited higher self-healing capability compared to the conventional binder.

Based on the findings presented in section 9, Table 6 summarizes the effects of various asphalt modifiers on their fatigue lives.

10. Conclusions

This review paper provides a comprehensive overview of the evaluation of the fatigue life of asphalt binders, covering the testing methods, the failure criteria, the failure definitions, the effect of testing conditions as well as the effect of bitumen penetration grade, chemical composition, and bitumen modification. Based on the reported findings, the following conclusions and recommendations are drawn.

- The linear amplitude sweep (LAS) test has become the preferred testing method for evaluating fatigue life of asphalt binders since its introduction. It offers advantages such as accelerated testing compared to the time sweep (TS) test.
- Various failure criteria and definitions are used to predict the fatigue life of asphalt binders using both LAS and TS tests. In particular, the viscoelastic continuum damage (VECD) concept is widely utilized for analyzing LAS test results, incorporating both dissipated energy and pseudo-strain energy. The S-VECD and G^R approach has emerged

Table 6 – Effect of some additives on the fatigue life of asphalt binders.

	SBS	CR	Nanoparticles*	Sasobit®	Date seed ash	Graphene oxide	Diatomite	WEO+PPA	Bio-oil
Positive effect	•	•	•	•	•	•		•	•
Negative effect							•		

Note: * nanoparticles include carbon nanotubes, nanoclays, organo-montmorillonite, nano-hydrated lime.

as the most recommended method for analyzing LAS test results due to its independence from loading history, loading mode, and temperature effects.
- The temperature of the fatigue test significantly affects asphalt binder fatigue life. Different methods for selecting test temperatures exist, but there is no consensus on the optimal temperature. Further research is needed to standardize temperature selection.
- The impact of chemical composition on fatigue life remains complex and contradictory. While softer binders generally exhibit higher fatigue resistance. More research is needed to understand the relationships between chemical composition and fatigue behavior.
- Polymer-modified binders generally exhibit superior fatigue performance compared to conventional binders. Additives such as crumb rubber and styrene-butadiene-styrene (SBS) contribute positively to the fatigue life of asphalt binders. Additionally, elastomeric modified asphalt demonstrates higher fatigue resistance compared to non-elastomeric binders.

Therefore, it is recommended to utilize the LAS test on PAV-aged bitumen under strain-controlled conditions, employing the S-VECD and G^R approach. Additionally, fatigue testing should be conducted at an intermediate reference temperature adapted to the climate zone of each country or region.

Conflict of interest

The authors do not have any conflict of interest with other entities or researchers.

REFERENCES

AASHTO, 2014. Standard Method of Test for Estimating Damage Tolerance of Asphalt Binders Using the Linear Amplitude Sweep. AASHTO TP 101-14. American Association of State Highway and Transportation Oficials, Washington DC.

AASHTO, 2015. Standard Specification for Performance-Graded Asphalt Binder. AASHTO M 320. American Association of State Highway and Transportation Officials (AASHTO), Washington DC.

AASHTO, 2016. Standard Method of Test for Measuring Asphalt Binder Yield Energy and Elastic Recovery Using the Dynamic Shear Rheometer. AASHTO TP 123-16. American Association of State Highway and Transportation Oficials, Washington DC.

AASHTO, 2021. Standard Method of Test for Estimating Damage Tolerance of Asphalt Binders Using the Linear Amplitude Sweep. AASHTO T 391-20. American Association of State Highway and Transportation Oficials, Washington DC.

Adhikari, S., Shen, S., You, Z., 2009. Evaluation of fatigue models of hot-mix asphalt through laboratory testing. Transportation Research Record 2127, 36–42.

Ahmed, T.M., Al-Khalid, H., Ahmed, T.Y., 2019. Review of techniques, approaches and criteria of hot-mix asphalt fatigue. Journal of Materials Civil Engineering 31 (12), 03119004.

Airey, G.D., Rahimzadeh, B., 2004. Combined bituminous binder and mixture linear rheological properties. Construction and Building Materials 18 (7), 535–548.

Alae, M., Zhao, Y., Zarei, S., et al., 2020. Effects of layer interface conditions on top-down fatigue cracking of asphalt pavements. International Journal of Pavement Engineering 21 (3), 280–288.

Ameri, M., Seif, M.R., Abbasi, M., et al., 2017. Viscoelastic fatigue resistance of asphalt binders modified with crumb rubber and styrene butadiene polymer. Petroleum Science and Technology 35, 30–36.

An, X., Wang, R., Kang, X., et al., 2023. A more accurate fatigue characterization of GO-modified asphalt binder considering non-linear viscoelastic behaviour and UV exposure effects. International Journal of Fatigue 168, 107396.

Anderson, D.A., Le Hir, Y.M., Marasteanu, M.O., et al., 2001. Evaluation of fatigue criteria for asphalt binders. Transportation Research Record 1766, 48–56.

Asadi, B., Tabatabaee, N., Hajj, R., 2021. Use of linear amplitude sweep test as a damage tolerance or fracture test to determine the optimum content of asphalt rejuvenator. Construction and Building Materials 300, 123983.

Aurilio, M., Tavassoti, P., Elwardany, M., et al., 2021. Impact of Styrene-Butadiene-Styrene (SBS) content on asphalt Binder's fatigue resistance at various aging levels using Viscoelastic Continuum Damage and fracture mechanics. Construction and Building Materials 305, 124627.

Baglieri, O., Tsantilis, L., Santagata, E., 2018. Evaluation of healing potential of bituminous binders using a viscoelastic continuum damage approach. Construction and Building Materials 184, 344–350.

Bahia, H.U., Zeng, M., Khatri, M.A., et al., 2001. Characterization of Modified Asphalt Binders in Superpave Mix Design. Transportation Research Board, Washington DC.

Basueny, A., Carter, A., Perraton, D., 2015. Complex modulus and fatigue performance of a GB20 mix incorporating 40 percent reclaimed asphalt pavement. In: Sixtieth Annual Conference of the Canadian Technical Asphalt Association, Ottawa, 2015.

Bessa, I.S., Vasconcelos, K.L., Castelo Branco, V.T.F., et al., 2019. Fatigue resistance of asphalt binders and the correlation with asphalt mixture behaviour. Road Materials and Pavement Design 20, S695–S709.

Błażejowski, K., Wójcik-Wiśniewska, M., Baranowska, W., et al., 2020. Fatigue performance of bituminous binders tested by linear amplitude sweep test. In: Pasetto, M., Partl, M.N., Tebaldi, G. (Eds.), Proceedings of the 5th International Symposium on Asphalt Pavements & Environment (APE), Lecture Notes in Civil Engineering. Springer International Publishing, Cham, pp. 385–394.

Bonnetti, K.S., Nam, K., Bahia, H.U., 2002. Measuring and defining fatigue behavior of asphalt binders. Transportation Research Record 1810, 33–43.

Boussabnia, M.M., Perraton, D., Lamothe, S., et al., 2021. Evaluation of the effect of the loading frequency on Wöhler's curve parameters of a high modulus asphalt. Road Materials and Pavement Design 23 (9), 2151–2166.

Canestrari, F., Ingrassia, L.P., 2020. A review of top-down cracking in asphalt pavements: causes, models, experimental tools and future challenges. Journal of Traffic and Transportation Engineering (English Edition) 7 (5), 541–572.

Canestrari, F., Virgili, A., Graziani, A., et al., 2015. Modeling and assessment of self-healing and thixotropy properties for modified binders. International Journal of Fatigue 70, 351–360.

Cao, W., Wang, C., 2018. A new comprehensive analysis framework for fatigue characterization of asphalt binder using the Linear Amplitude Sweep test. Construction and Building Materials 171, 1–12.

Cao, W., Wang, C., 2019. Fatigue performance characterization and prediction of asphalt binders using the linear amplitude sweep based viscoelastic continuum damage approach. International Journal of Fatigue 119, 112–125.

Chehab, G., Kim, Y.R., Schapery, R.A., et al., 2002. Time-temperature superposition principle for asphalt concrete mixtures with growing damage in Tension State. Journal of the Association of Asphalt Paving Technologists 71, 559–593.
Chen, H., Bahia, H.U., 2022. Proposed asphalt binder fatigue criteria for various traffic conditions using the LAS or the G-R parameters. Materials and Structures 55, 24.
Chen, M., Geng, J., Chen, H., et al., 2021. Effect of water aging on the fatigue performance of asphalt binders using the linear amplitude sweep. Construction and Building Materials 304, 124679.
Chen, H., Zhang, Y., Bahia, H.U., 2022. Modelling asphalt binder fatigue at multiple temperatures using complex modulus and the LAS test. International Journal of Pavement Engineering 23 (13), 4600–4609.
de Oliveira, L.S., Babadopulos, L.F.A.L., Soares, J.B., 2021. Evolution of asphalt binder stiffness during fatigue loading and rest periods and its impact on fatigue life. International Journal of Fatigue 144, 106041.
Deef-Allah, E., Abdelrahman, M., 2021. Investigating the relationship between the fatigue cracking resistance and thermal characteristics of asphalt binders extracted from field mixes containing recycled materials. Transportation Engineering 4, 100055.
Di Benedetto, H., de La Roche, C., Baaj, H., et al., 2004. Fatigue of bituminous mixtures. Materials and Structures 37 (3), 202–216.
Garcia, D.C., Faxina, A.L., Leonel, E.D., 2020. A tool based on the linear elastic fracture mechanics to analyze the outputs of the linear amplitude sweep (LAS) test. Construction and Building Materials 264, 120255.
Gaudenzi, E., Cardone, F., Lu, X., et al., 2020. Analysis of fatigue and healing properties of conventional bitumen and bio-binder for road pavements. Materials 13 (2), 420.
Ghuzlan, K.A., Carpenter, S.H., 2000. Energy-derived, damage-based failure criterion for fatigue testing. Transportation Research Record 1723, 141–149.
Ghuzlan, K.A., Carpenter, S.H., 2006. Fatigue damage analysis in asphalt concrete mixtures using the dissipated energy approach. Canadian Journal of Civil Engineering 33 (7), 890–901.
Hajj, R., Bhasin, A., 2018. The search for a measure of fatigue cracking in asphalt binders–a review of different approaches. International Journal of Pavement Engineering 19, 205–219.
Hammoum, F., de La Roche, C., Piau, J.M., et al., 2002. Experimental investigation of fracture and healing of bitumen at pseudo-contact of two aggregates. In: 9th International Conference on Asphalt Pavement, Copenhagen, 2002.
Hintz, C., 2012. Understanding Mechanisms Leading to Asphalt Binder Fatigue (PhD thesis). University of Wisconsin-Madison, Madison.
Hintz, C., Bahia, H., 2013. Simplification of linear amplitude sweep test and specification parameter. Transportation Research Record 2370, 10–16.
Hintz, C., Velasquez, R., Johnson, C., et al., 2011. Modification and validation of linear amplitude sweep test for binder fatigue specification. Transportation Research Record 2207, 99–106.
Hopman, P.C., Kunst, P.A.J.C., Pronk, A.C., 1989. A renewed interpretation method for fatigue measurements, verification of miner's rule. In: 4th Eurobitume Symposium, Copenhagen, 1989.
Jia, H., Sheng, Y., Guo, P., et al., 2023. Effect of synthetic fibers on the mechanical performance of asphalt mixture: a review. Journal of Traffic and Transportation Engineering (English Edition) 10 (3), 331–348.
Johnson, C., 2010. Estimating Asphalt Binder Fatigue Resistance Using an Accelerated Test Method (PhD thesis). University of Wisconsin-Madison, Madison.
Johnson, C., Bahia, H.U., 2010. Evaluation of an accelerated procedure for fatigue characterization of asphalt binders. Road Materials and Pavement Design 10, 1–26.
Johnson, C., Wen, H., Bahia, H.U., 2009. Practical application of viscoelastic continuum damage theory to asphalt binder fatigue characterization. Asphalt Paving Technology 78, 597–638.
Joohari, I.B., Giustozzi, F., 2022. Oscillatory shear rheometry of hybrid polymer-modified bitumen using multiple stress creep and recovery and linear amplitude sweep tests. Construction and Building Materials 315, 125791.
Kamboozia, N., Saed, S.A., Rad, S.M., 2021. Rheological behavior of asphalt binders and fatigue resistance of SMA mixtures modified with nano-silica containing RAP materials under the effect of mixture conditioning. Construction and Building Materials 303, 124433.
Kavussi, A., Barghabany, P., 2016. Investigating fatigue behavior of nanoclay and nano hydrated lime modified bitumen using LAS test. Journal of Materials in Civil Engineering 28 (3), 04015136.
Kim, Y.R., Little, D.N., Lee, H.J., 2006. A simple testing method to evaluate fatigue fracture and damage performance of asphalt mixtures. Journal of the Association of Asphalt Paving Technology 71, 176–206.
Kuchiishi, A.K., Carvalho, J.P.B., Bessa, I.S., et al., 2019. Effect of temperature on the fatigue behavior of asphalt binder. Applied Rheology 29, 30–40.
Lee, H.-J., Kim, Y.R., 1998. Viscoelastic continuum damage model of asphalt concrete with healing. Journal of Engineering Mechanics 124 (11), 1224–1232.
Lefeuvre, Y., 2001. Etude Expérimentale et Modélisation De La Fissuration De Matériaux Bitumineux (PhD thesis). Ecole Nationale des Ponts et Chaussées, Paris.
Li, L., Wu, C., Cheng, Y., et al., 2022. Laboratory investigation on viscoelastic and fatigue properties of diatomite modified asphalt based on dynamic shear rheometer. Construction and Building Materials 327, 126940.
Liu, G., van de Ven, M., Wu, S., et al., 2011. Influence of organo-montmorillonites on fatigue properties of bitumen and mortar. International Journal of Fatigue 33 (12), 1574–1582.
Liu, H., Luo, R., Huang, T., 2019. Development of failure criterion and fatigue model to characterize the fatigue resistance of asphalt binders under controlled-stress time sweep tests. In: Transportation Research Board 98th Annual Meeting, Washington DC, 2019.
Liu, Z., Li, S., Wang, Y., 2022. Waste engine oil and polyphosphoric acid enhanced the sustainable self-healing of asphalt binder and its fatigue behavior. Journal of Cleaner Production 339, 130767.
Luo, Y., Guo, P., Gao, J., et al., 2022. Application of design-expert response surface methodology for the prediction of rejuvenated asphalt fatigue life. Journal of Cleaner Production 379, 134427.
Lyu, L., Wang, Z., Ji, J., et al., 2022. Investigating rheological and healing properties of asphalt binder modified by disulfide-crosslinked poly(urea-urethane) elastomer. Construction and Building Materials 347, 128546.
Maillard, S., 2002. Comportement du bitume en film mince sous chargement répété. In: The 9ème Colloque de la Recherche de l'intergroupe des Ecoles Centrales, Nantes, 2002.
Mannan, U.A., Tarefder, R.A., 2018. Investigating different fatigue failure criteria of asphalt binder with the consideration of healing. International Journal of Fatigue 114, 198–205.

Mannan, U.A., Islam, M.R., Tarefder, R.A., 2015. Effects of recycled asphalt pavements on the fatigue life of asphalt under different strain levels and loading frequencies. International Journal of Fatigue 78, 72–80.
Martono, W., Bahia, H.U., 2008. Developing a surrogate test for fatigue asphalt binders. In: 87th Transportation Research Board Annual Meeting, Washington DC, 2008.
Martono, W., Bahia, H.U., D'Angelo, J., 2007. Effect of testing geometry on measuring fatigue of asphalt binders and mastics. Journal of Materials in Civil Engineering 19, 746–752.
Mirhosseini, A.F., Kavussi, A., Kamali, M.H.J., et al., 2017. Evaluating fatigue behavior of asphalt binders and mixes containing date seed ash. Journal of Civil Engineering Management 23 (8), 1164–1175.
Morshed, M.M.T., Hossain, Z., Chen, D.-H., et al., 2020. Exploration of alternatives of elastic recovery and conventional fatigue tests of modified binders. International Journal of Pavement Research and Technology 13 (6), 630–636.
Nan, H., Sun, Y., Chen, J., et al., 2022. Investigation of fatigue performance of asphalt binders containing SBS and CR through TS and LAS tests. Construction and Building Materials 361, 129651.
NCHRP, 2021. Relationships Between the Fatigue Properties of Asphalt Binders and the Fatigue Performance of Asphalt Mixtures. NCHRP-982. National Cooperative Highway Research Program, Washington DC.
O'Connell, J., Mturi, G.A.J., Komba, J., et al., 2017. Analysis of the binder yield energy test as an indicator of fatigue behaviour of asphalt mixes. IOP Conference Series: Materials Science and Engineering 236, 012012.
Park, S.W., Kim, Y.R., Schapery, R.A., 1996. A viscoelastic continuum damage model and its application to uniaxial behavior of asphalt concrete. Mechanics of Materials 24 (4), 241–255.
Pereira, A., Micaelo, R., Quaresma, L., et al., 2016. Evaluation of different methods for the estimation of the bitumen fatigue life with DSR testing. RILEM Bookseries 11, 1017–1028.
Perraton, D., Baaj, H., Benedetto, H.D., et al., 2003. Évaluation de la résistance à la fatigue des enrobés bitumineux fondée sur l'évolution de l'endommagement du matériau en cours d'essai: aspects fondamentaux et application à l'enrobé à matrice de pierre. Canadian Journal of Civil Engineering 30 (5), 902–913.
Piau, J.M., 1989. Thermomechanical modelling of the behavior of bituminous mixes. Bulletin De Liaison Des Laboratoires Ponts ET Chaussées 163, 41–55.
Planche, J.-P., Anderson, D.A., Gauthier, G., et al., 2004. Evaluation of fatigue properties of bituminous binders. Materials and Structures 37, 356–359.
Pronk, A.C., Hopman, P.C., 1991. Energy dissipation: the leading factor of fatigue. In: Highway Research: Sharing the Benefits, London, 1990.
Qiu, X., Cheng, W., Xu, W., et al., 2020. Fatigue evolution characteristic and self-healing behaviour of asphalt binders. International Journal of Pavement Engineering 23 (5), 1459–1470.
Raithby, K.D., Sterling, A.B., 1972. Some Effects of Loading History on the Fatigue Performance of Rolled Asphalt. Transport and Road Research Laboratory, Wokingham. 29.
Reese, R., 1997. Properties of aged asphalt binder related to asphalt concrete fatigue life. Journal of the Association of Asphalt Paving Technology 66, 604–632.
Roque, R., Yan, Y., Lopp, G., 2020. Cracking Performance Evaluation of Asphalt Binders at Intermediate Temperatures. BDV31-977-83. Florida Department of Transportation, Tallahassee.
Rowe, G.M., Bouldin, M.G., 2000. Improved techniques to evaluate the fatigue resistance of asphaltic mixtures. In: 2nd Eurasphalt and Eurobitume Congress, Barcelona, 2000.
Saboo, N., Kumar, P., 2016. Performance characterization of polymer modified asphalt binders and mixes. Advances in Civil Engineering 2016, 5938270.
Sabouri, M., Kim, Y.R., 2014. Development of a failure criterion for asphalt mixtures under different modes of fatigue loading. Transportation Research Record 2447, 117–125.
Sabouri, M., Mirzaiyan, D., Moniri, A., 2018. Effectiveness of linear amplitude sweep (LAS) asphalt binder test in predicting asphalt mixtures fatigue performance. Construction and Building Materials 171, 281–290.
Safaei, F., Castorena, C., 2016. Temperature effects of linear amplitude sweep testing and analysis. Transportation Research Record 2574, 92–100.
Safaei, F., Castorena, C., 2017. Material nonlinearity in asphalt binder fatigue testing and analysis. Materials & Design 133, 376–389.
Safaei, F., Castorena, C., 2020. Improved interpretation of asphalt binder parallel plate dynamic shear rheometer fatigue tests. International Journal of Pavement Engineering 21 (1), 74–87.
Safaei, F., Castorena, C., Kim, Y.R., 2016. Linking asphalt binder fatigue to asphalt mixture fatigue performance using viscoelastic continuum damage modeling. Mechanics of Time-Dependent Materials 20 (3), 299–323.
Salehfard, R., Behbahani, H., Dalmazzo, D., et al., 2021. Effect of colloidal instability on the rheological and fatigue properties of asphalt binders. Construction and Building Materials 281, 122563.
Santagata, E., Baglieri, O., Dalmazzo, D., et al., 2009. Rheological and chemical investigation on the damage and healing properties of bituminous binders. Journal of the Association of Asphalt Paving Technology 78, 567–596.
Santagata, E., Baglieri, O., Tsantilis, L., et al., 2015. Fatigue and healing properties of nano-reinforced bituminous binders. International Journal of Fatigue 80, 30–39.
Schapery, R.A., 1984. Correspondence principles and a generalized J integral for large deformation and fracture analysis of viscoelastic media. International Journal of Fracture 25 (3), 195–223.
Schapery, R.A., 1990. A theory of mechanical behavior of elastic media with growing damage and other changes in structure. Journal of the Mechanics and Physics of Solids 38 (21), 215–253.
Schapery, R.A., Park, S.W., 1999. Methods of interconversion between linear viscoelastic material functions. Part II—an approximate analytical method. International Journal of Solids and Structures 36, 1677–1699.
Shen, S., Sutharsan, T., 2011. Quantification of cohesive healing of asphalt binder and its impact factors based on dissipated energy analysis. Road Materials and Pavement Design 12 (3), 525–546.
Shen, S., Airey, G.D., Carpenter, S.H., et al., 2006. A dissipated energy approach to fatigue evaluation. Road Materials and Pavement Design 7 (1), 47–69.
Shen, S., Chiu, H.-M., Huang, H., 2010. Characterization of fatigue and healing in asphalt binders. Journal of Materials in Civil Engineering 22 (9), 846–852.
Shenoy, A., 2002. Fatigue testing and evaluation of asphalt binders using the dynamic shear rheometer. Journal of Testing and Evaluation 30 (4), 303–312.
Shi, C., Zhou, W., Wang, T., et al., 2022. Fatigue performance characterization of styrene-butadiene-styrene and crumb rubber composite modified asphalt binders with high crumb rubber contents. Journal of Cleaner Production 331, 129979.
Steineder, M., Peyer, M.J., Hofko, B., et al., 2022. Comparing different fatigue test methods at asphalt mastic level. Materials and Structures 55 (5), 132.

Sudarsanan, N., Kim, Y.R., 2022. A critical review of the fatigue life prediction of asphalt mixtures and pavements. Journal of Traffic and Transportation Engineering (English Edition) 9 (5), 808–835.

Sun, D., Yu, F., Li, L., et al., 2017. Effect of chemical composition and structure of asphalt binders on self-healing. Construction and Building Materials 133, 495–501.

Sun, Y., Wang, W., Chen, J., 2019. Investigating impacts of warm-mix asphalt technologies and high reclaimed asphalt pavement binder content on rutting and fatigue performance of asphalt binder through MSCR and LAS tests. Journal of Cleaner Production 219, 879–893.

Tabatabaee, N., Tabatabaee, H.A., 2010. Multiple stress creep and recovery and time sweep fatigue tests: crumb rubber modified binder and mixture performance. Transportation Research Record 2180, 67–74.

Underwood, B.S., 2016. A continuum damage model for asphalt cement and asphalt mastic fatigue. International Journal of Fatigue 82, 387–401.

Underwood, B.S., Kim, Y.R., Guddati, M.N., 2006. Characterization and performance prediction of alf mixtures using a viscoelastoplastic continuum damage model. Journal of the Association of Asphalt Paving Technology 75, 577–636.

Van Dijk, W., Moreaud, H., Quedeville, A., et al., 1972. The fatiguee of bitumen and bituminous mixes. In: 3rd International Conference on the Structural Design of Asphalt Pavements, London, 1972.

Wang, C., Castorena, C., Zhang, J., et al., 2015. Unified failure criterion for asphalt binder under cyclic fatigue loading. Road Materials and Pavement Design 16, 125–148.

Wang, C., Zhang, H., Castorena, C., et al., 2016. Identifying fatigue failure in asphalt binder time sweep tests. Construction and Building Materials 121, 535–546.

Wang, X., Su, Z., Xu, A., et al., 2017. Shear fatigue between asphalt pavement layers and its application in design. Construction and Building Materials 135, 297–305.

Wang, C., Xie, W., Chen, Y., et al., 2018a. Refining the calculation method for fatigue failure criterion of asphalt binder from linear amplitude sweep test. Journal of Materials in Civil Engineering 30, 04017286.

Wang, C., Xie, W., Underwood, B.S., 2018b. Fatigue and healing performance assessment of asphalt binder from rheological and chemical characteristics. Materials and Structures 51 (6), 171.

Wang, C., Chen, Y., Xie, W., 2020. A comparative study for fatigue characterization of asphalt binder using the linear amplitude sweep test. Materials and Structures 53, 95.

Wang, C., Chen, Y., Gong, G., 2021. Cohesive and adhesive healing evaluation of asphalt binders by means of the LASH and BBSH tests. Construction and Building Materials 282, 122684.

Wang, C., Gong, G., Ren, Z., 2022. Addressing the healing compensation on fatigue damage of asphalt binder using TSH and LASH tests. International Journal of Fatigue 167, 107292.

Wang, C., Sun, Y., Ren, Z., 2023. Toward to a viscoelastic fatigue and fracture model for asphalt binder under cyclic loading. International Journal of Fatigue 168, 107479.

Xie, W., Castorena, C., Wang, C., et al., 2017. A framework to characterize the healing potential of asphalt binder using the linear amplitude sweep test. Construction and Building Materials 154, 771–779.

Yan, Y., Hernando, D., Park, B., et al., 2021. Understanding asphalt binder cracking characterization at intermediate temperatures: review and evaluation of two approaches. Construction and Building Materials 312, 125163.

Yan, C., Yuan, L., Yu, X., et al., 2022. Characterizing the fatigue resistance of multiple modified asphalts using time sweep test, LAS test and elastic recovery test. Construction and Building Materials 322, 125806.

Yang, K., Li, R., Underwood, B.S., et al., 2022. Effect of laboratory oxidative aging on dynamic shear rheometer measures of asphalt binder fatigue cracking resistance. Construction and Building Materials 337, 127566.

Yang, K., Cui, H., Ma, X., et al., 2023. Understanding and characterizing the fatigue cracking resistance of asphalt binder at intermediate temperature: a literature review. Construction and Building Materials 407, 133432.

Yue, M., Yue, J., Wang, R., et al., 2021. Evaluating the fatigue characteristics and healing potential of asphalt binder modified with Sasobit® and polymers using linear amplitude sweep test. Construction and Building Materials 289, 123054.

Zeiada, W., Liu, H., Ezzat, H., et al., 2022. Review of the Superpave performance grading system and recent developments in the performance-based test methods for asphalt binder characterization. Construction and Building Materials 319, 126063.

Zhang, Z., Oeser, M., 2021a. Energy dissipation and rheological property degradation of asphalt binder under repeated shearing with different oscillation amplitudes. International Journal of Fatigue 152, 106417.

Zhang, Z., Oeser, M., 2021b. Understanding the damage mechanism of asphalt binder under controlled-stress fatigue loads in dynamic shear rheometer. Construction and Building Materials 292, 123463.

Zhang, J., Sabouri, M., Guddati, M.N., et al., 2013. Development of a failure criterion for asphalt mixtures under fatigue loading. Road Materials and Pavement Design 14, 1–15.

Zhang, H., Shen, K., Xu, G., et al., 2020. Fatigue resistance of aged asphalt binders: an investigation of different analytical methods in linear amplitude sweep test. Construction and Building Materials 241, 118099.

Zhang, R., Sias, J.E., Dave, E.V., 2022. Development of new performance indices to evaluate the fatigue properties of asphalt binders with ageing. Road Materials and Pavement Design 23 (2), 377–396.

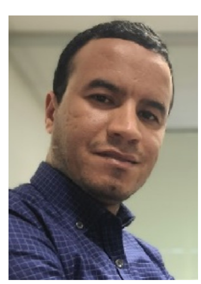

Dr. Mohammed Nouali is an assistant professor at the Research Center of ESTP (Grande école d'ingénieurs de la construction) in France. He received his civil engineering degree in 2013, followed by a magister degree in 2016, and completed his PhD in civil engineering in 2021. His research interests revolve around the fatigue of asphalt mixtures and binders, thermal and photo-oxidative aging of asphalt binders, and the mechanical behavior of asphalt mixtures, including those containing reclaimed asphalt pavement. Additionally, he is involved in research on plastic waste-modified asphalt binders.

Dr. Anne Dony is an associate professor in the Research Center of ESTP (Grande école d'ingénieurs de la construction) in Cachan near Paris, in the team of materials for sustainable construction. She is the head of the bituminous materials laboratory and of the IRAUD (road infrastructure and sustainable urban development) teaching chair. A chemist by training, she has worked in the field of pavement materials for over 30 years. She focuses her research on the performance and durability of pavement materials, the development of alternative materials, recycling of bituminous materials and warm techniques, mainly using experimental approaches, with industrial partnerships and participation in national and international collaborative projects.

Mr. Alan Carter is a professor in construction engineering at the École de Technologie Supérieure (ÉTS) since 2005. He obtained his bachelor's and master's degrees at ÉTS, and his doctorate at Auburn University (NCAT), where he worked on asphalt recycling. His research focuses on pavement materials and pavement design. He mainly works on hot and cold asphalt recycling, mix design and characterization of asphalt materials, and empirical mechanistic pavement design. With over 100 publications as author or co-author, professor Carter also heads the pavement and bituminous materials laboratory (LCMB) at ÉTS.